공학석사 학위논문

Structural effect of different Pebax/ZIF-8 MMMs on CO_2 permeability

이산화탄소 기체투과에 미치는 다른 Pebax/ZIF-8 MMMs 의 구조적 영향

2019 년 8 월

서울대학교 대학원

에너지시스템공학부

김 지 인

Structural effect of different Pebax/ZIF−8 MMMs on CO_2 permeability

지도 교수 정 은 혜

이 논문을 공학석사 학위논문으로 제출함

2019 년 8 월

서울대학교 대학원

에너지시스템공학부

김 지 인

김지인의 공학석사 학위논문을 인준함

2019 년 8 월

위 원 장 _____ (인)

부위원장 _____ (인)

위 원 _____ (인)

Abstract

The CO_2 separation by membrane technology has been investigated by many researchers because of its environmental and economic benefit. Among many kinds of membrane, the mixed matrix membranes (MMMs) has showed enhancement of both gas permeability and selectivity by combining polymeric membrane and inorganic fillers to improve not only gas transport but also mechanical strength and adsorption of particular gas molecules.

Pebax 1657 and Pebax 2533 based MMMs were prepared by controlling molar ratio of nanoparticle ZIF-8 precursors, 2-methylimidazole (2-MeIM) and zinc nitrate hexahydrate (Zn). Three different types of ZIF-8 were synthesized by controlling molar ratio of 2-MeIM/ Zn by 2/1, 8/1, and 32/1. The SEM images and XRD patterns of ZIF-8 showed that particles sizes and crystallinity peak were decreased as molar ratio of ZIF-8 increased. Three types of ZIF-8 particles were dispersed on both Pebax 1657 and 2533 and resulting solution of Pebax/ZIF-8 were casted on Teflon dish for 72 h at 50 ˚C.

Prepared Pebax 1657/ZIF-8 and Pebax 2533/ZIF-8 with different molar ratio 2-MeIM/ Zn of 2/1, 8/1, and 32/1 were used for single CO_2 and N_2 gas permeation test at increasing temperature of 15, 35, 55, and 75 ˚C. At the same temperature, the highest CO_2 permeability was observed for Pebax 1657/ZIF-8 with 2-MeIM/Zn molar ratio of 32/1 and Pebax 2533/ZIF-8 with 2-MeIM/Zn molar ratio of 2/1. The highest permeabilities of Pebax 1657 MMMs and Pebax 2533 MMMs with different molar ratio of 2-MeIM/Zn were confirmed by XRD patterns of Pebax/ZIF-8 MMMs. From the XRD patterns, for Pebax 1657 MMMs, molar ratio 2-MeIM/Zn of 32/1 showed the lowest crystallinity, and for Pebax 2533 MMMs,

molar ratio 2-MeIM/Zn of 2/1 showed the lowest crystallinity, which has the least obstacle for gas permeation.

The CO_2 permeability of Pebax 2533/ZIF-8 was higher than that of Pebax 1657/ZIF-8, however, CO_2/N_2 selectivity was higher in Pebax 1657/ZIF-8 than Pebax 2533/ZIF-8. At increasing temperature of permeation test, Pebax 1657/ZIF-8 and Pebax 2533/ZIF-8 showed the enhancement of CO_2 and N_2 permeability, and since both CO_2 and N_2 permeability increased, the CO_2/N_2 selectivity decreased as temperature increased.

Different results of the CO_2 permeability and the CO_2/N_2 selectivity of Pebax 1657/ZIF-8 and Pebax 2533/ZIF-8 MMMs were explained by comparing content of polyethylene (PE) and polyamide (PA) segment in Pebax, chemical interaction between ZIF-8 and Pebax, and chemical nature of CO_2 affinity of Pebax. In this study, the effect of ZIF-8 types on CO_2 permeability of two types of Pebax/ZIF-8 MMMs was investigated to confirm important factor of compatibility of Pebax and ZIF-8 and to find the optimal condition of Pebax/ZIF-8 for CO_2 permeability.

Keywords: Pebax 1657, Pebax 2533, Molar ratio controlling ZIF-8, Mixed matrix membranes, CO_2 capture

Student Number: 2017-22704

Contents

List of Tables

List of Figures

Chapter 1. Introduction

1.1 Background

The use of fossil fuel has increased the concentration of gaseous CO_2 in the atmosphere, which has led to the greenhouse effect (Xu et al., 2016; Koros and Lively, 2012). CO_2 can be captured using various mixtures such as natural gas or flue-gas through conventional technologies like absorption with solvents and cryogenic CO_2 capture (Xu et al., 2016; Koros and Lively, 2012). However, these methods are being replaced by membrane technologies because of their low cost and energy efficiency (Rezakazemi et al., 2014). Generally, polymeric membranes have been applied to gas separation processes in industry because they consume low energy, have low cost, and are environmentally sustainable (Nafisi et al., 2014). Especially, rubbery polymers, such as poly(dimethyl siloxane) (PDMS) and poly(cis-isoprene), have been applied to CO_2 gas separation, because efficient gas transport can be achieved by flexile and soft chain mobility, resulting higher permeability than glassy polymers (Bondar et al., 2000; Sutrisna et al., 2017). In the rubbery polymer, polar ether groups are significant components for achieving high CO_2 permeability and reasonable efficient CO_2/nonpolar gas selectivity because of their high affinity to CO_2 (Nafisi et al., 2014). Recent studies have reported that incorporation of poly(ether oxide) (PEO) segment with other monomers can be used to overcome the weakness of fragile PEO segments to improve the weak mechanical strength (Lin and Freeman, 2005; Okamoto et al., 1995). Polyether block polyamide copolymers (Pebax) are widely studied for CO_2 separation because they are flexible, durable, and mechanically and thermally resistant. Furthermore, they show high selectivity of CO_2 over nonpolar gases such as N_2 and CH_4 (Zheng et al., 2018).

Pebax is composed of thermoplastic polyamide (PA) segment and rubbery polyether (PE) segment (Jomekian et al., 2016). PA is a rigid and hard crystalline phase that provides mechanical strength to a Pebax membrane (Nordin et al., 2015). PE is a flexible and soft amorphous phase that provides high CO_2 permeability through its high affinity for polar molecules, which makes it feasible to select polar gases from non-polar gases like N_2 (Aroon et al., 2010). Specifically, PA segment contains polyamide 12 (nylon-12) and polyamide 6 (nylon-6) and PE segment contains poly(tetramethylene oxide) (PTMEO) and poly(ethylene oxide) (PEO) (Bondar et al., 2000). Bondar et al. (2000) and Kim et al. (2001) compared Pebax series by chemical composition and structures, their melting points of PA and PE, glass-transition point of PA and PE, and crystallinity (Table 1). Therefore, CO_2 permeability shows different values based on Pebax series. In PE groups in Pebax, PEO groups more polar than PTMEO, so that Pebax containing PEO groups have more cohesive energy density, and therefore gas diffusion is lower than Pebax containing PTMEO. Therefore, Pebax 2533 (80% of PTMEO and 20% of PA12) (Figure 1B) shows higher permeability than Pebax 1657 (60% of PEO and 40% of PA6) (Figure 1A) because it has higher content of PE, which is highly associated with gas transport, and it also has PTMEO, instead of PEO, which has higher diffusivity. However, Pebax 1657 shows higher CO_2/N_2 selectivity than Pebax 2533, because PEO segment in Pebax 1657 has higher affinity to CO_2 than PTEMO segment in Pebax 2533. PA content in Pebax corresponds to the crystallinity region in polymeric matrix in Pebax, which directly affects decrease of permeability as PA loading increases. Kim et al. (2001) performed CO_2 and N_2 permeation by Pebax 1657 with increasing temperature from 25, 45, 65, and 85 ˚C. As temperature increased, the permeability of both CO_2 and N_2 increased, resulting in decrease of selectivity of CO_2/N_2.

Table 1 Chemical properties of Pebax series (Bondar et al., 2000; Kim et al., 2001)

Pebax series	Chemical structure	Density (g/cm^3)	T_m(PE) (°C)	T_m(PA) (°C)	Crystallinity of PA block (wt.%)	Reference
2533	80PTMEO/20PA12	1.01	10	126	14	Bondar et al.
3533	70PTMEO/30PA12	1.01	18	155	20	Kim et al.
4033	54PTMEO/46PA12	1.01	21	180	30	Bondar et al.
1657	60PEO/40PA6	1.14	49	204	25	Kim et al.
1074	55PEO/45PA6	1.14	11	156	40	Bondar et al.

A

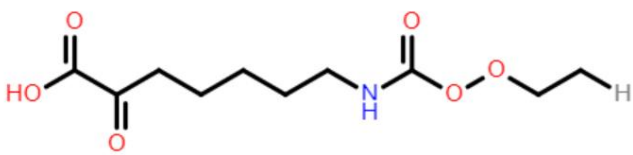

B

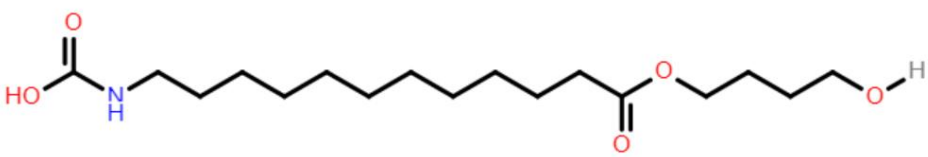

Figure 1 (A) Pebax 1657 chemical structure (B) Pebax 2533 chemical structure

The Robeson upper bound is the empirical upper bound relationship between the permeability of a specific component of a gas mixture and the separation factor and was defined by Lloyd M. Robeson. As the separation factor decreases, the permeability of more permeable gas components increases in a trade-off relationship (Robeson, 2008). However, based on Robeson's upper bound, the CO_2

permeability of polymeric membrane increases, while the CO_2 selectivity decreases (Robeson, 2008). This drawback of polymeric membranes can be overcome by combining highly permeable polymers with inorganic fillers, which can increase gas selectivity while maintaining high permeability for CO_2 (Sutrisna et al., 2017).

To improve permeability and mitigate the loss of selectivity, inorganic fillers are dispersed in polymeric membranes to produce hybrid membranes called mixed matrix membranes (MMMs). The fillers include zeolites, carbon molecular sieves, and inorganic particles like silica and TiO_2 (Jomekian et al., 2016). However, conventional inorganic fillers have weak adhesion with organic polymer (Xu et al., 2017). For sustainable fabrication of MMMs, metal organic frameworks (MOFs) have been introduced as porous materials composed of metal ion liked to organic likers, which provide high surface area that adsorbs affinitive gas molecules (Sutrisna et al., 2017).

Zeolitic imidazolate frameworks are a subclass of MOFs, which include zinc metal cations and 2-methylimidazole anions of organic linkers that form a six-membered ring (Nafisi et al., 2014). ZIFs have a special molecular sieving effect that provides strong interfacial interaction with polymers (Song et al., 2012; Dong et al., 2013). ZIFs are used as a membrane supplement for CO_2 capture since they have high thermal and chemical stability, and their micro-pore size of 3.4 Å is suitable for gas transport of CO_2, which has a kinetic diameter of 3.3 Å (Zheng and Ding, 2018). Precursors of ZIF-8, zinc nitrate hexahydrate, and 2-methylimidazole are well fabricated on a polymeric matrix of PA segment in Pebax, which makes permeation easier for CO_2 gas molecules of higher polarizability (29.1×10^{25} cm^3) compared to N_2 gas molecules of lower polarizability (17.4×10^{25} cm^3) (Sutrisna et al., 2017).

1.2 Literature review

In recent years, ZIF-8 coated Pebax MMMs have been tested for CO_2 gas separation with other gases such as N_2, O_2, and CH_4. Xu et al. (2017) prepared Pebax 1657/ZIF-8 MMMs to investigate that permeability of CO_2 improved by 300% compared to pure Pebax 1657, and selectivities of CO_2/CH_4 and CO_2/N_2 were very close to the Robeson upper bound. Also, the effect of temperature on separation of CO_2, N_2, and CH_4 was performed, which permeability of all gases increased whereas selectivity decreased. Jomekian et al. (2016) reported preparing Pebax 1657/ZIF-8 MMMs supported by polyethersulfone (PES) sub layer enhanced the mechanical strength for Pebax thin layer and prevented resistance for gas flux. CO_2 permeability and CO_2/CH_4 selectivity of Pebax 1657/ZIF-8/PES with both Pebax of 1 wt.% and 4 wt.% were improved as the synthesized temperature of ZIF-8 particle temperature increased from 30, 40, 50 to 60˚C. However, Pebax 1657/ZIF-8/PES membrane with Pebax 4 wt.% showed lower permeability but higher selectivity because of thicker selective layer. Sutrisna et al. (2017) compared two types of Pebax 1657/ZIF-8 MMMs of dense film flat sheet and hollow fibre membrane coated with highly permeable poly[1-(trimethylsilyl)-1-propyne] (PTMSP) gutter layer. Compared to pure Pebax 1657, Pebax 1657/ZIF-8 MMMs flat sheet improved CO_2 permeability by 176%. With increased pressure, CO_2 permeability slightly decreased because CO_2 molecules are less adsorbed on the surface of membrane and polymer chain is compacted with increasing pressure. The selectivity of CO_2/CH_4 of pure pebax 1657 decreased significantly, whereas Pebax 1657/ZIF-8 MMMs selectivity was relatively unchanged when pressure increased. With the hollow fibre composite membrane, gas permeability increased with addition of ZIF-8 loading, which showed higher permeability than flat sheet membrane of Pebax 1657/ZIF-8. Also, hollow fibre composite membrane had

effect of long-term stability, which CO_2 gas permeance had been maintained reasonable amount of permeability and operated by 16 days. Nafisi et al. (2014) investigated CO_2, CH_4, N_2, and O_2 gas separation by Pebax 2533 membrane with loading of 0% to 40% of ZIF-8 using dry feed and humidified feed. CO_2 permeability of Pebax 2533/ZIF-8 with 40% loading at dry mixed gas was improved by 584% compared to pure Pebax 2533, however CO_2/N_2 selectivity dropped 50.8%. However in humidified mixed gas condition, CO_2 permeability of Pebax 2533/ZIF-8 with 50% loading at humidified mixed gas was improved by 499% compared to pure Pebax 2533, whereas less CO_2/N_2 selectivity dropped 67.3%. Nafisi et al. (2014) concluded that incorporation of ZIF-8 dropped CO_2/N_2 selectivity both in dry feed and humidified feed because of porous structure of inorganic ZIF-8 layer on Pebax 2533 polymeric matrix.

One of important factor of successful fabrication of MMMs is enhancing interface compatibility between inorganic filler ZIF-8 and organic polymer Pebax membrane (Jomekian et al., 2017). To achieve interfacial volume but no defect on MMMs, size controlling technique of inorganic filler has been modified on membrane fabrication. Jomekian et al. (2017) modified Pebax 1657/ZIF-8 MMMs with increasing molar ratio of ZIF-8 precursors to decrease ZIF-8 particle size, and also utilized ionic liquids on the surface of MMMs. CO_2 permeability of Pebax 1657/ZIF-8 MMMs was improved by 166, 180, and 193% as ZIF-8 particle size decreased compared to pure Pebax 1657. Also, CO_2/N_2 selectivity increased and slightly unchanged with decreasing of ZIF-8 particle, when other studies showed that selectivity of CO_2/N_2 decreased as simply increasing ZIF-8 loading.

Mostly studied research have reported the results of CO_2 permeability and CO_2/nonpolar gases selectivity of Pebax 1657/ZIF-8 MMMs by either increasing ZIF-8 particle loading, controlling feed pressure of permeation test, or fabricating membrane with support layer such as PTMSP gutter layer and ionic liquid-

modification. However, even though Pebax 2533 has shown high CO_2 permeability compared to other Pebax series, Pebax 2533/ZIF-8 MMMs have not been studied as much as Pebax 1657/ZIF-8 MMMs. Recently, ZIF-8 particle size controlling technique has been gradually introduced to improve CO_2 permeability of Pebax 1657/ZIF-8 MMMs, however, this technique has not been widely studied so that the mechanisms and reasons for permeability improvement of MMMS have not been explained in detail. Also, ZIF-8 particle size-controlling technique has not been applied to Pebax 2533/ZIF-8 MMMs in recent studies.

1.3 Research objective

The main purpose of this research is to discover relationship between Pebax 1657 and ZIF-8 and between Pebax 2533 and ZIF-8 with controlling molar ratio of ZIF-8 precursors, and to compare CO_2 permeability and CO_2/N_2 selectivity of Pebax 1657/ZIF-8 MMMs and Pebax 2533/ZIF-8 MMMs. Pebax 2533 is known to be the most efficient copolymer for CO_2 permeation, and Pebax 1657 has been widely used for MMMs with ZIF-8, which is why they were chosen to find the optimal conditions for Pebax/ZIF-8 MMMs. Also, size-controlling technique was applied for Pebax 2533/ZIF-8 MMMs to determine whether the CO_2 permeability results show similar or different trend compared to that of 1657/ZIF-8 MMMs.

In this study, three conditions were applied on CO_2 and N_2 gas permeation, which were two different Pebax series membranes Pebax 1657 and Pebax 2533, three different types of ZIF-8 particles by controlling molar ratio of precursors, and four increasing permeating temperature. Comparison between Pebax 1657/ZIF-8 and Pebax 2533/ZIF-8 explained how chemical structure, interfacial interaction of particle-polymer, and chemical bonding of polymer and nanoparticle influence the CO_2 permeability. Lastly, the effect of increasing temperature on both Pebax 1657/ZIF-8 and Pebax 2533/ZIF-8 was tested to compare CO_2 permeability and CO_2/N_2 selectivity difference when temperature increases.

Chapter 2. Materials and Methods

2.1. Synthesis of ZIF-8 particles

ZIF-8 nanoparticles were synthesized with different molar ratios of the precursors 2-methylimidazole (99%, 2-MeIM) and zinc nitrate hexahydrate (99%, $Zn(NO_3)_2 \cdot 6H_2O$) (Merck, Inc.). The molar ratios of 2-MeIM/$Zn(NO_3)_2 \cdot 6H_2O$ (2-MeIM/Zn) were set as 2/1, 8/1, and 32/1 (Jomekian et al., 2017; Jomekian et al., 2016). Furthermore, 0.55, 2.2, and 8.8 g of 2-MeIM were used with 1 g of $Zn(NO_3)_2 \cdot 6H_2O$ to obtain molar ratios of ZIF-8 particles of 2/1, 8/1, and 32/1, respectively. Each precursor was dissolved in 200 ml of methanol (99.99%, MeOH) separately. A cloudy solution was obtained after vigorous stirring for 1 h. The obtained solution was centrifuged for 1 h at 5000 rpm to separate the synthesized ZIF-8 particles from the methanol solution. The deposited ZIF-8 powder was prepared by pouring methanol solution and drying at ambient temperature for 24 h.

2.2. Preparation of Pebax/ZIF-8 MMMs

Pebax 1657 and Pebax 2533 were provided by Arkema, Inc. Pebax 1657 and Pebax 2533 were dissolved at 3 wt.% in a solution of ethanol (99.99%, EtOH)/deionized water (70 wt.%/30 wt.%) at 75 ˚C for 2 h and in butanol (99.99% BuOH) at 80 ˚C for 3 h, respectively. Next, 10 wt.% of each of the three different ZIF-8 powders molar ratios 2/1, 8/1, and 32/1 were added based on the ZIF-8

loading equation (Eq. (1)). ZIF-8 powder (Figure 2) was dispersed in the prepared solutions by an ultrasonication bath for 10 min. The Pebax/ZIF-8 MMM film (Figure 2) was prepared in Teflon dishes and dried in a vacuum oven at 50 ˚C for 72 h.

$$\text{ZIF-8 loading (wt.\%)} = \frac{m_{ZIF-8}}{m_{Pebax}+m_{ZIF-8}} \times 100\ \% \qquad (1)$$

Figure 2 ZIF-8 powder (left) and Pebax/ZIF-8 MMM film (right)

2.3. Permeability test

Gas permeation tests with a single gas (CO_2 or N_2) were performed using a flat sheet module at constant volume. The single gas tests were performed at a feed pressure of 3 bar and increasing temperatures of 15, 35, 55, and 75˚C. The CO_2 and N_2 permeabilities were calculated with the various temperatures of the feed gas while maintaining differences of pressure between the feed side and permeate side based on the following equation:

$$P = \frac{VL}{ART\,(p_{feed}-p_{permeate})}\left(\frac{dp_{permeate}}{dt}\right) \qquad (2)$$

where P is the permeability of CO_2 and N_2 (Barrer, 1 Barrer = 10^{-10} cm^3 (STP) cm cm^{-2} s^{-1} $cmHg^{-1}$), V is the volume of the permeate side of the membrane (cm^3), L is the thickness of the membrane (cm), p_{feed} is the pressure of the feed, $p_{permeate}$ is the pressure of the permeate (cmHg s^{-1}), T is the varied temperature of the feed side (K), A is the membrane area (cm^2), $\frac{dp_{permeate}}{dt}$ is the rate of pressure of the permeate side (cmHg s^{-1}), and R is the ideal gas constant (0.278 cmHg cm^3 cm^{-3} (STP) K^{-1}). The permeation selectivity of CO_2 and N_2 was calculated using the permeability ratio (Eq. (3)) of the more permeable gas (CO_2) to the less permeable gas (N_2).

$$\alpha_{CO_2/N_2} = \frac{P_{CO_2}}{P_{N_2}} \qquad (3)$$

2.4. Characterization

The particle size distribution of ZIF-8 particles in deionized water was analyzed by Zetasizer (Nano ZS90, Malvern, USA). FE-SEM (JSM-7800F Prime, JEOL Ltd, Japan) at 10-15 kV was used to characterize the size and morphology of the ZIF-8 nanoparticles and to obtain surface and cross-sectional images of Pebax 1657/ZIF-8 MMM and Pebax 2533/ZIF-8 MMM. Powder X-ray diffraction (XRD) (SmartLab, Rigaku, Japan) was performed on the ZIF-8 nanoparticles, pure Pebax, and Pebax/ZIF-8 MMM to determine the crystallinity. XRD was applied with Cu K_α radiation (40 kV-40 mA) at a scan speed of 2˚/min and step size of 0.02˚ by scanning 2θ angles between 5˚ and 60˚.

A differential scanning calorimeter (DSC) (Discovery DSC, TA Instrument, USA) was used to determine the thermal properties of pure Pebax and Pebax/ZIF-8 MMM at a temperature range of -70 to 230 ˚C at a scanning rate of 10 ˚C /min. Thermogravimetric analysis (TGA) (Discovery TGA, TA Instrument, USA) was used to determine the weight changes of ZIF-8 particles, pure Pebax 1657, Pebax 2533, and Pebax/ZIF-8 MMMs as a function of temperature over time. Simultaneously, TGA was performed with a temperature range of 0 to 600 ˚C and a heating rate of 10 ˚C/min for Pebax 1657 and Pebax 2533, while a temperature range of 0 to 900 ˚C and a heating rate of 10 ˚C/min were used for ZIF-8 particles. Fourier transform infrared spectroscopy (FTIR) (Nicolet 6700, Thermo Scientific, USA) was used to confirm the new bond formation between ZIF-8 and the surface of the polymeric matrix in Pebax 1657 and Pebax 2533. FTIR was used with a wavenumber range of 650 cm^{-1} to 4000 cm^{-1}, an average of 32 scans, and resolution of 8.

Chapter 3. Results and Discussion

3.1. Characterization of ZIF-8

The SEM images and particle size distributions of ZIF-8 (Figure 3) were analyzed to compare size and shape of ZIF-8 particles of different molar ratio of precursors. As molar ratio of 2-MeIM/Zn increased, the size of ZIF-8 particle decreased. The results of decreasing size of ZIF-8 with increasing molar ratio of ZIF-8 precursors were also described by Jomekian et al (2016). Size distributions of Z2, Z8, and Z32 ranged from 295.3 nm to 712.4 nm, 220.2 nm to 531.2 nm, and 105.7 nm to 458.7 nm, respectively. The average size of Z2, Z8, and Z32 were 500.7, 363.3, and 217.1 nm, respectively.

The X-ray diffraction results of each ZIF-8 with increasing molar ratio of 2-MeIM/Zn were prepared to characterize the crystallinity of ZIF-8 structure (Figure 4). As molar ratios of 2-MeIM/Zn increased, the intensity of characteristic XRD peaks decreased, and the peak becomes wider. The decrease of XRD peaks with increasing 2-MeIM/Zn was resulted from excess of MeIM (Zhang et al., 2018). The excess MeIM on the particle surface prevent from particle growth, resulting in decrease of crystallinity (Zhang et al., 2018). Furthermore, the XRD pattern obtained with decreasing molar ratio of 2-MeIM/Zn showed higher and narrower peaks (Zheng and Ding, 2018). It means ZIF-8 with decreasing molar ratio has high crystallinity (Zheng and Ding, 2018). This can be characterized by the Scherrer equation (Eq. (4)), in which the peak width is inversely proportional to the crystal size:

$$B(2\theta) = \frac{K\lambda}{L\cos\theta} \qquad (4)$$

where B is the peak width, K is the constant of proportionality, called the Scherrer constant, θ is the Bragg angle, and L is the crystallite size. K depends on the shape and size distribution of the crystals and varies from 0.62 to 2.08 (Balzar et al., 2004). L increases at large 2θ, whereas the peak intensity becomes weaker (Balzar et al., 2004). The narrow peaks and high intensity indicate crystalline particles, whereas broader peaks and low intensity indicate amorphous particles. Therefore, the molar ratio of Z2 results in crystalline structure, whereas that of Z32 results in amorphous structure.

The TGA graph of ZIF-8 shows the rate of change in weight of ZIF-8 as a function of temperature (Figure 5). The weight loss of Z32 was faster than that of Z2 and Z8 around 150 ˚C. The slope of weight loss of all three ZIF-8 at 200-600 ˚C decreased steadily, which represents the range of adsorbed water evaporation and decomposition of residual ligand (Zheng et al., 2018). Then, all of ZIF-8 was completely decomposed at range of 600-900 ˚C, which agrees to TGA data of ZIF-8 reported by Zheng et al. (2018). Decomposition of ZIF-8 particles at high temperature corresponds that ZIF-8 particles are thermally stable (Zheng et al., 2018).

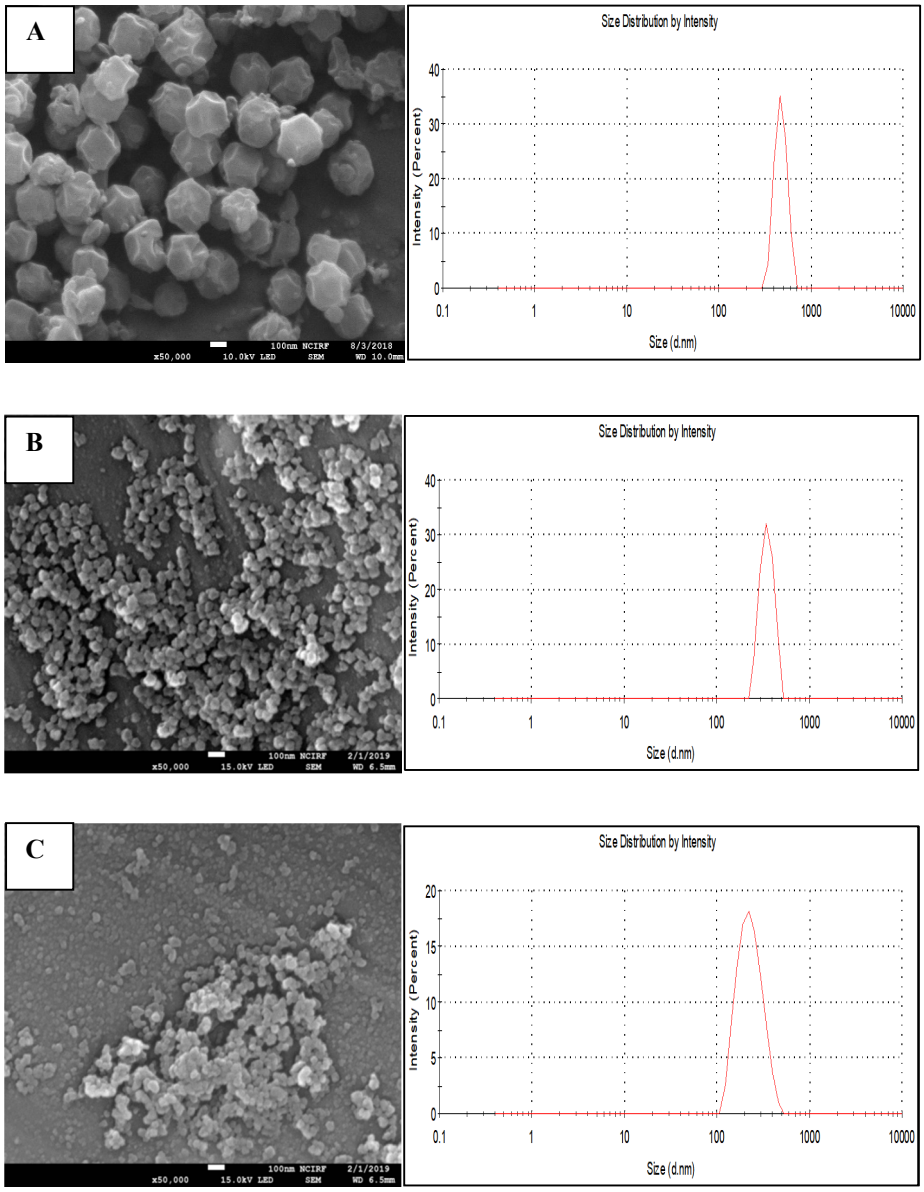

Figure 3 SEM images and size distributions of ZIF-8 particles with different 2-MeIM/Zn (A) Z2, (B) Z8, and (C) Z32

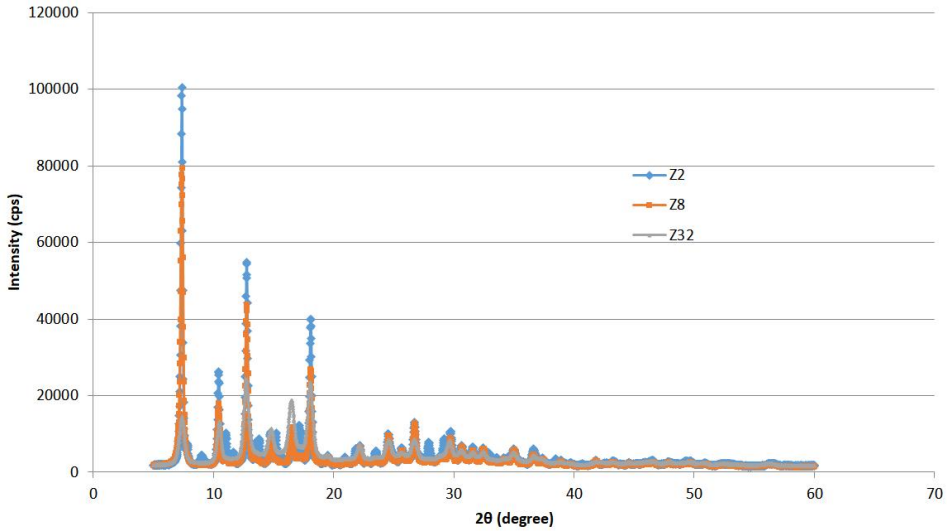

Figure 4 XRD of ZIF-8 particles with different 2-MeIM/Zn

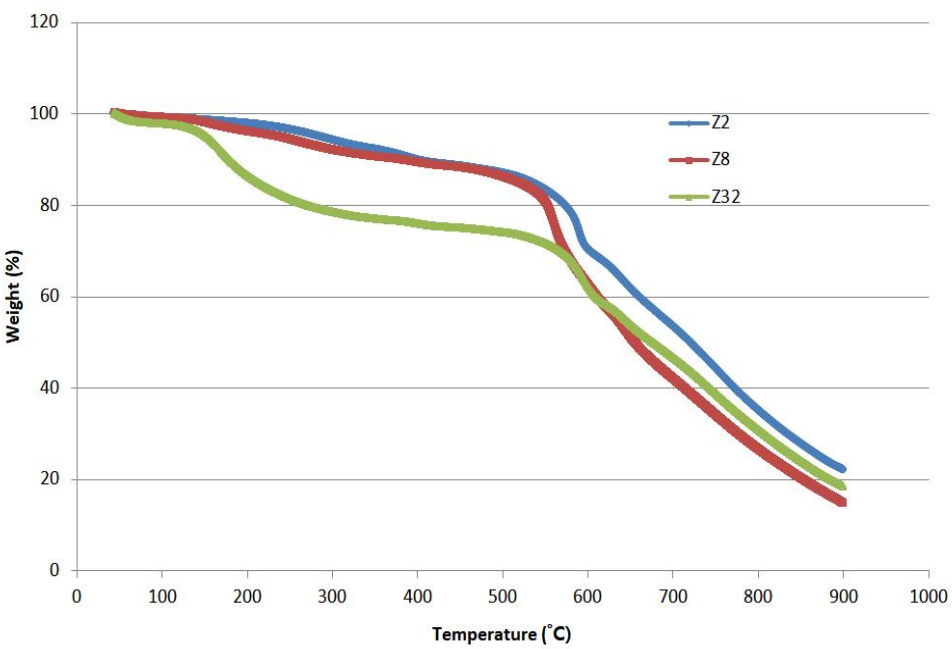

Figure 5 TGA of ZIF-8 particles with different 2-MeIM/Zn

3.2. Characterization of Pebax/ZIF-8 MMMs

There was a similar trend of decreasing size of ZIF-8 nanoparticles embedded in the polymeric matrix in SEM images of the surface and cross section of the Pebax 1657/ZIF-8 (Figure 6) and Pebax 2533/ZIF-8 (Figure 7) with increasing molar ratio of ZIF-8. Table 2 represents the abbreviated names of all Pebax/ZIF-8 MMMs with different 2-MeIM/Zn of ZIF-8. When Z2 was used in P1 and P2, there was space between each Z2 particle (red circle in Figure 6B and 7B) between each Z2 particles. The connections of the Pebax matrix were shown between Z2 particles, which indicate good interfacial interaction between the ZIF-8 particles and Pebax (yellow arrow in Figure 6B and 7B). On the other hand, as the molar ratio increased from Z2 and Z8 to Z32 in P1 and P2, there was less space between the ZIF-8 particles and less connection between them and the Pebax.

Table 2 The abbreviated names of all Pebax/ZIF-8 MMMs with different 2-MeIM/Zn of ZIF-8

Full name of Pebax/ZIF-8 MMM	Abbreviated name of MMM
Pebax 1657/ZIF-8 2/1M	P1/Z2
Pebax 1657/ZIF-8 8/1M	P1/Z8
Pebax 1657/ZIF-8 32/1M	P1/Z32
Pebax 2533/ZIF-8 2/1M	P2/Z2
Pebax 2533/ZIF-8 8/1M	P2/Z8
Pebax 2533/ZIF-8 32/1M	P2/Z32

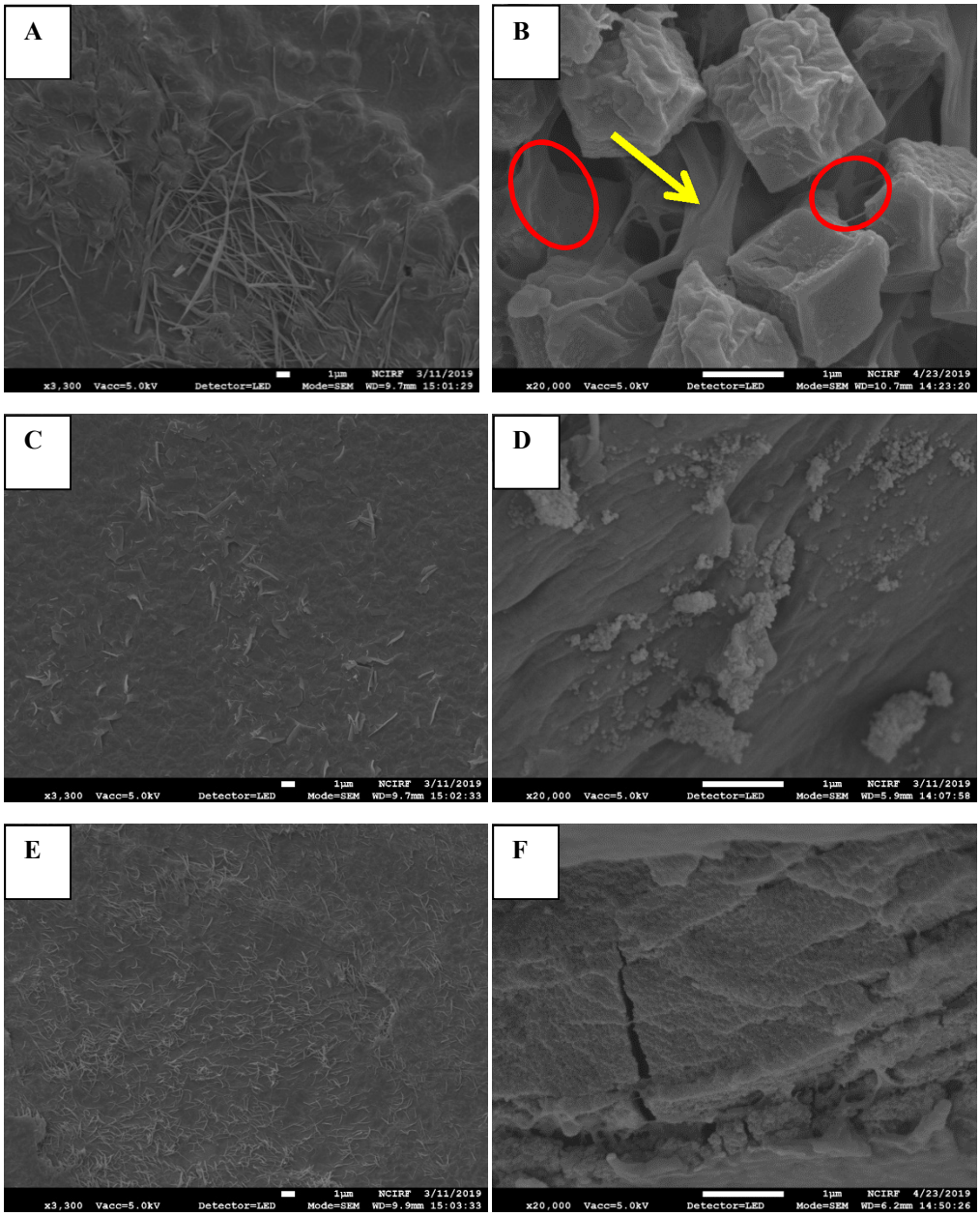

Figure 6 SEM image of surface (left) and cross-section (right) of P1/Z2 (A,B), P1/Z8 (C,D), and P1/Z32 (E,F)

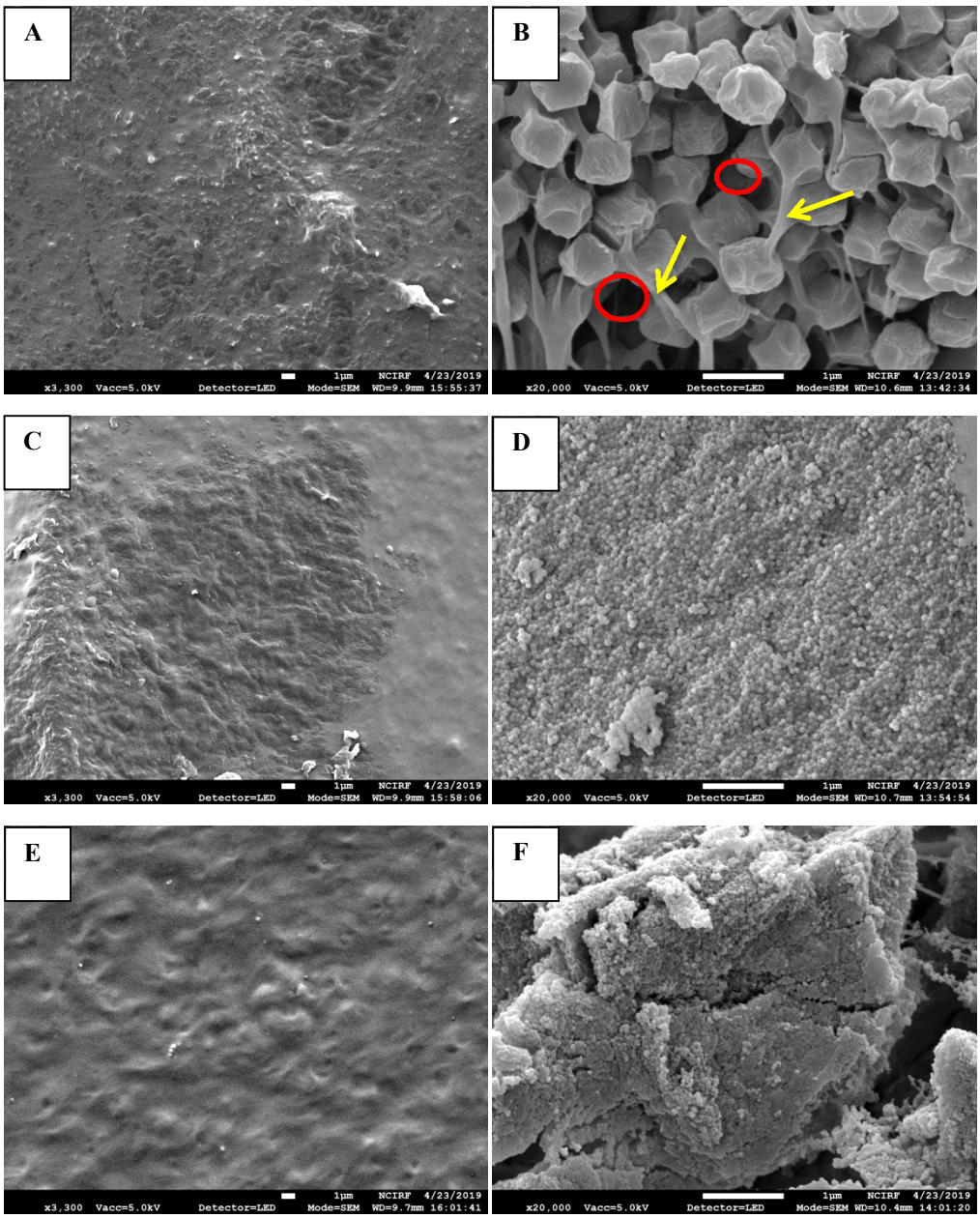

Figure 7 SEM image of surface (left) and cross-section (right) of P2/Z2 (A,B), P2/Z8 (C,D), and P2/Z32 (E,F)

P1 and P2 have significant difference in morphology (Figure 8). P1 showed straight rod-like shape and bended structure, which correspond to PA-6 segment and PEO segment, respectively (Sutrisna et al., 2017). On the other hand, P2 showed more uniform and flat surface rather than rod-like shape or bended shape.

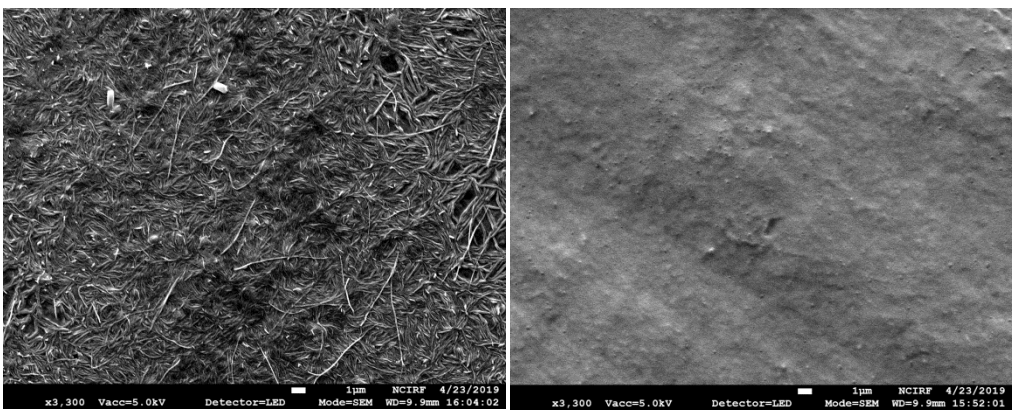

Figure 8 The SEM image of P1 (left) and P2 (right)

The FT-IR spectra of pure Pebax and Pebax/ZIF-8 MMM show the intensity of strongest absorption, which represents the stretching vibration of chemical bonds in membranes (Sutrisna et al., 2017; Nafisi and Hagg, 2014). Stretching vibration is the movement between two atoms held by shared electrons (Noller and Norman, 2019). Noller and Norman (2019) mentioned that two atoms vibrate back and forth, and maintain average bond length. Stretching vibration for each molecule has different energy level, which represents energy of wavelengths in infrared regions (Noller and Norman, 2019). For pure Pebax 1657, the peak at 1096.78 cm^{-1} represents the ether (-C-O-C-) group in the PEO segment, which is similar to the peak at 1094 cm^{-1} observed by Sutrisna et al. (2017). Sharp peaks at 3296.21, 1637.91, and 1737.31 cm^{-1} (Figure 9) represent the stretching vibration of -N-H- and H-N-C=O in saturated amide, and O-C=O in ester groups in the PA

segment in Pebax 1657 (Rabiee et al., 2015). The peak at 2937.22 cm^{-1} represents the stretching vibration of -C-H- bond in both the PEO segment and PA segment in Pebax 1657.

For pure Pebax 2533, the peak at 1105.43 cm^{-1} (Figure 10) represents the ether (-C-O-C-) group in the PEO segment. The sharp peaks at 3301.37, 1638.71, and 1734.20 cm^{-1} (Figure 10) represent the stretching vibration of -N-H- and H-N-C=O in saturated amide and O-C=O in ester groups in the PA segment in Pebax 2533. The peak at 2939.65 cm^{-1} (Figure 10) represents the stretching vibration of the -C-H- bond in both the PEO segment and PA segment in Pebax 2533. The similar spectra for pure Pebax and Pebax/ZIF-8 indicate that ZIF-8 particles are well connected to the PA segment of the Pebax matrix.

The connection between ZIF-8 particle and Pebax can be observed from SEM image of P1/Z2 and P2/Z2 (Figure 6B and 7B). When ZIF-8 particles disperse into polymer matrix, hydrogen bonding in PA segments is disrupted and new secondary hydrogen bonding is created at the interfacial space between ZIF-8 nanoparticle and Pebax polymer. There are hydrogen bonding between ZIF-8 and PA segments (Figure 11), which are between (1) aldehyde group in PA segment and methyl group in 2-methylimidazole in ZIF-8, and (2) N-H groups in PA and N atoms of imidazole ring (Sutrisna et al., 2017)

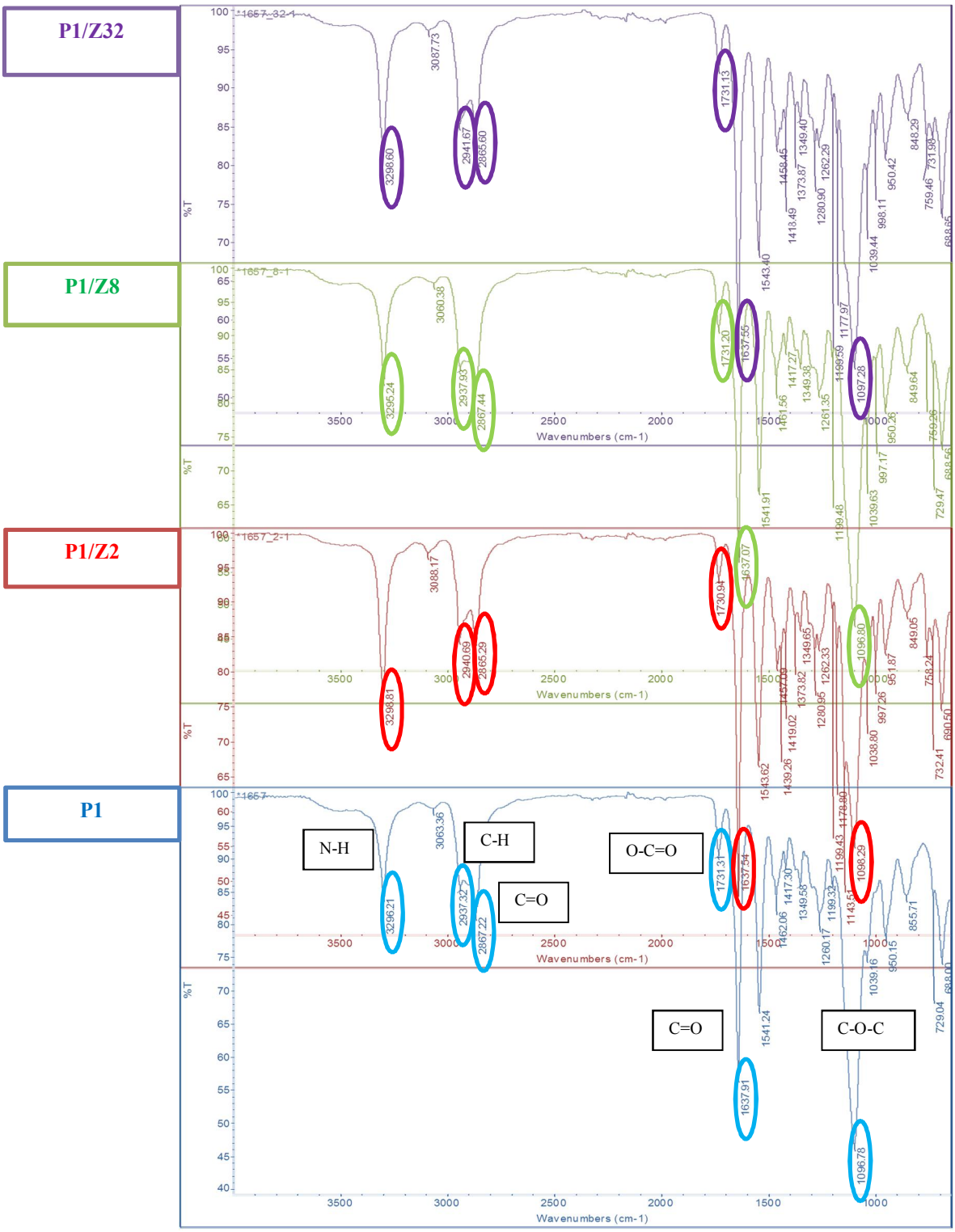

Figure 9 FT-IR spectra of P1, P1/Z2, P1/Z8, and P1/Z32

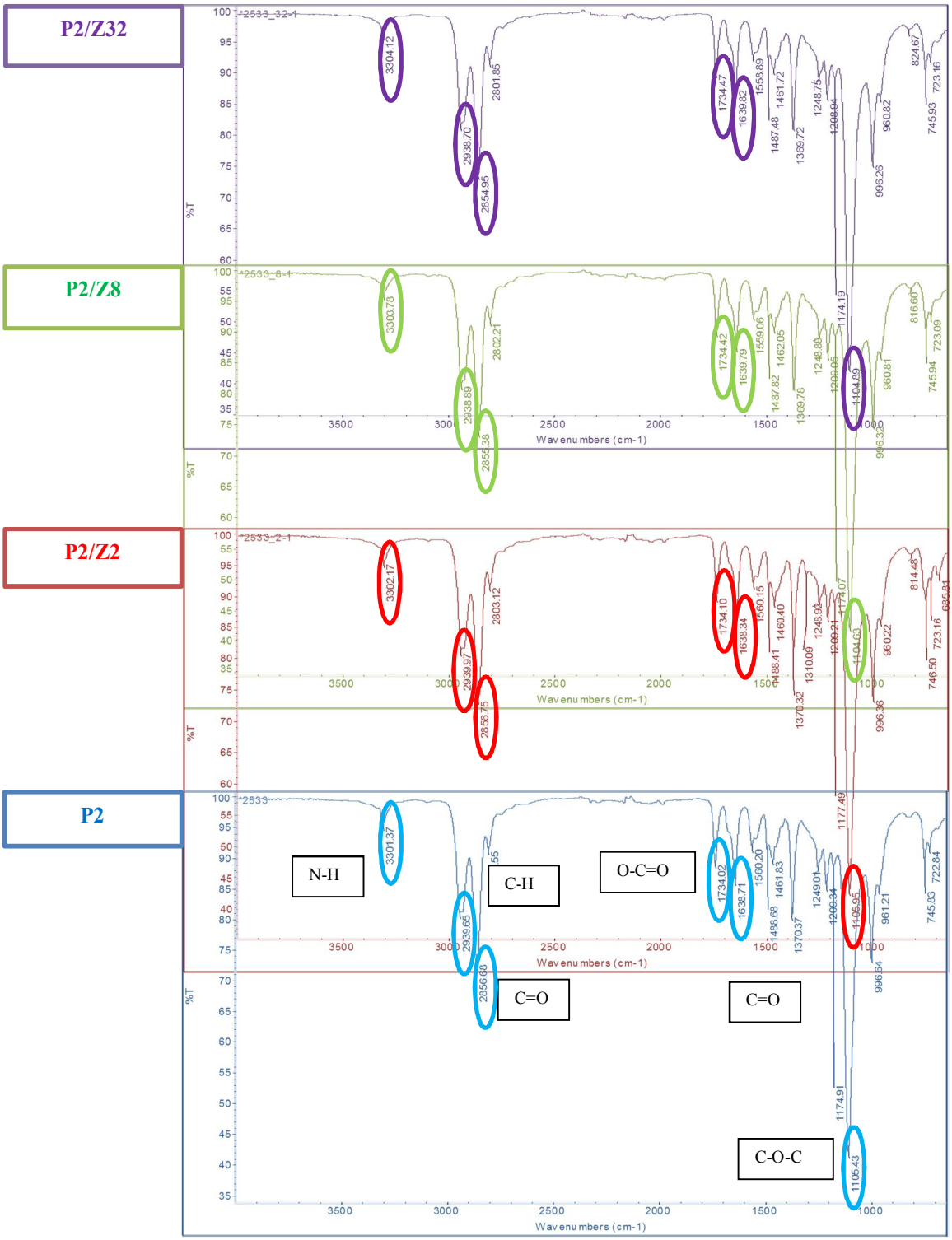

Figure 10 FT-IR spectra of P2, P2/Z2, P2/Z8, and P2/Z32

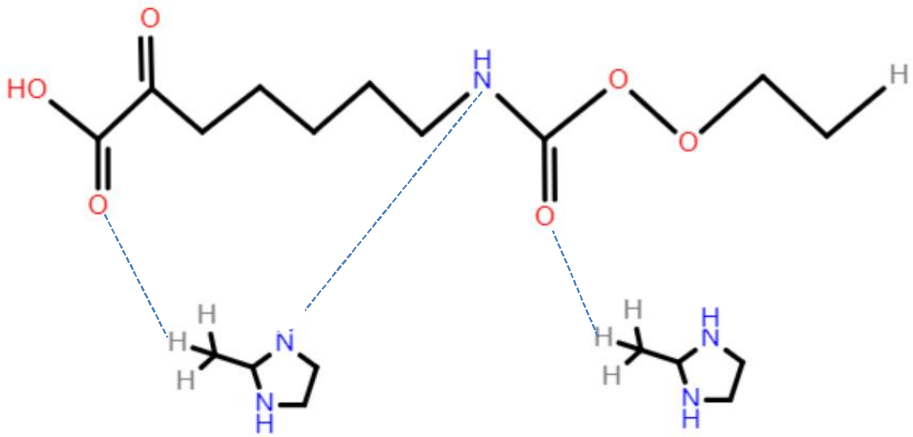

Figure 11 Hydrogen bonding of PA segment of Pebax 1657 and 2-methylimidazole in ZIF-8 particle (Sutrisna et al., 2017)

The XRD patterns of Pebax 1657/ZIF-8 MMMs and Pebax 2533/ZIF-8 MMMs show the crystallinity of both Pebax and ZIF-8 (Figure 12 and 13). In Figure 12, P1 shows a broad peak in the range of 16.8˚ to 22.7˚ and a sharp peak at 24˚, which represent of the amorphous PEO segment and crystalline PA segment, respectively. Distinct peaks of ZIF-8 in MMMs at 7.3˚, 10.4˚, 14.7˚, and 26.7˚were observed in the XRD pattern of Pebax 1657/ZIF-8, which were in good agreement with other studies. P1/Z2 showed the highest peak compared to P1/Z8 and P1/Z32. From the peak range of the PEO segment, (between 16.8˚ and 22.7˚), P1/Z32 showed the most similar pattern to P1 since Z32 has more amorphous structure than Z8 or Z2 (Figure 4). From the peak of the PA segment at 24˚, P1/Z2 showed more obvious and distinct PA peaks than P1/Z8 and P1/Z32 since Z2 has more crystalline structure than Z8 or Z32 (Figure 4).

In Figure 13, P2 showed peak at 20˚ for the crystalline PA segment, which agrees with previous work by Kim et al. (2001). Distinct peaks of ZIF-8 at 7.3˚,

10.4˚, and 14.7˚ were also observed in the pattern of Pebax 2533/ZIF-8 XRD. P2/Z2 showed the highest peak compared to P2/Z8 and P2/Z32, as in the XRD patterns of Pebax 1657/ZIF-8 MMM. However, after the peak at 16.3˚, P2/Z32 showed a significantly higher peak, whereas P2, P2/Z2, and P2/Z8 showed similar peaks.

Kim et al. (2001) reported that the crystallinity region in Pebax polymeric matrix affects permeability of Pebax to decrease because crystalline phase forms uniform and rigid chain which lacks in sorption sites and in mobility of chains to permeate penetrants. Therefore, from the XRD patterns, Pebax 1657 is more effective for permeating CO_2 with Z32, whereas Pebax 2533 is more effective for permeating CO_2 with Z2.

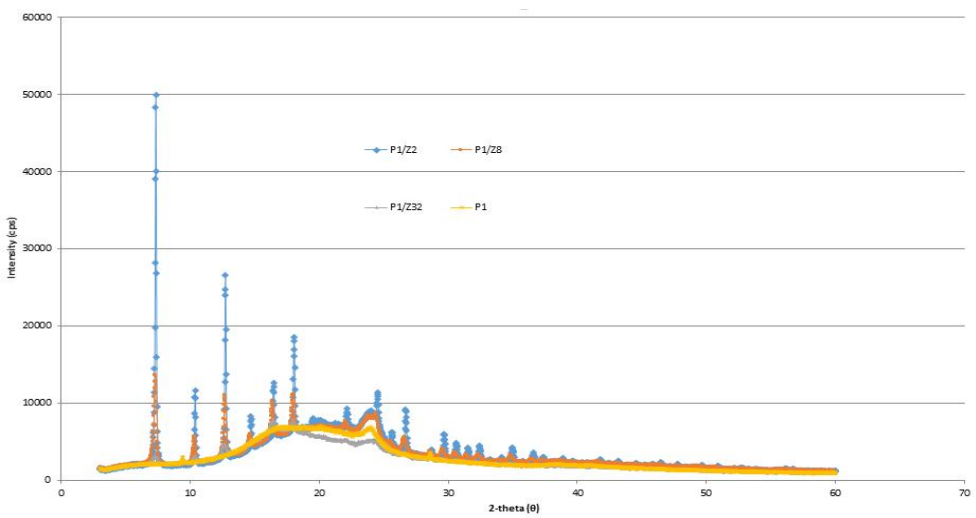

Figure 12 XRD patterns of Pebax 1657/ZIF-8 MMM with different 2-MeIM/Zn

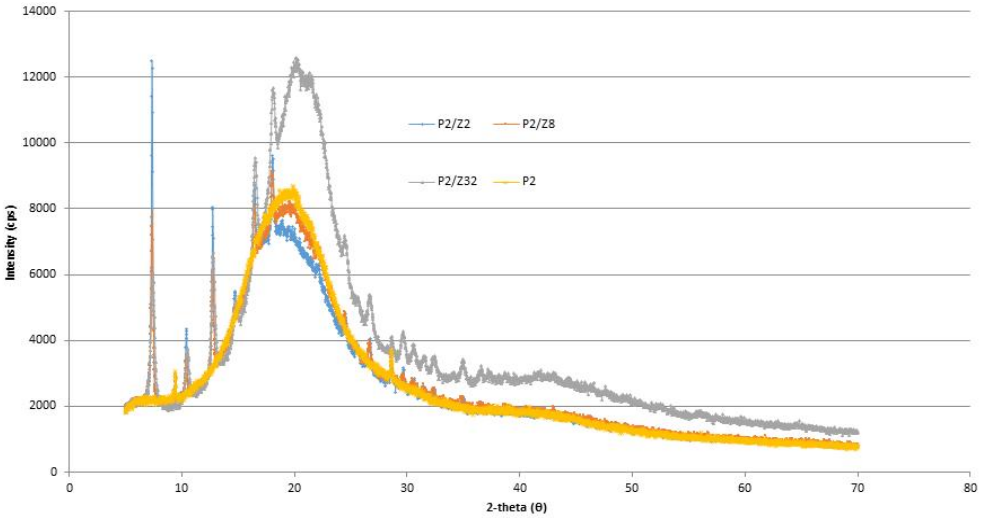

Figure 13 XRD patterns of Pebax 2533/ZIF-8 MMM with different 2-MeIM/Zn

The DSC curves were analyzed to determine the glass transition temperatures of PE and PA in the Pebax and Pebax/ZIF-8 MMMs. The polymer crystallinity was determined by measuring the enthalpy of fusion of the polymer (Wunderlich, 1990). Crystalline polymer shows higher enthalpy of fusion of polymer.

In Figure 14, exothermic peaks for PE segment and PA segment were observed as 12.42 ˚C and 204.097 ˚C for pure Pebax 1657, which agrees with the value reported in Zheng et al. (2018). These exothermic peaks correspond to melting point of PE and PA in Pebax 1657, which were 12 ˚C and 204 ˚C. As adding different molar ratio of ZIF-8 into Pebax 1657, peaks changed insignificantly because between each of ZIF-8 with different molar ratio and Pebax 1657 have similar weakness of interfacial interaction (Zheng et al., 2018). Even though peaks between Pebax 1657 and Pebax 1657/ZIF-8 MMM were similar, the enthalpy of PE in Pebax 1657 decreased the most in P1/Z32 from 17.701 J/g (Figure A4, see appendix) to 13.088 J/g (Figure A7). The enthalpy of PE decreased the most in P1/Z32 since Z32 could have changed the PE chain movement in the

interfacial region and created micro-voids in the polymeric matrix to a greater extent than other molar ratios of ZIF-8 (Figure 12).

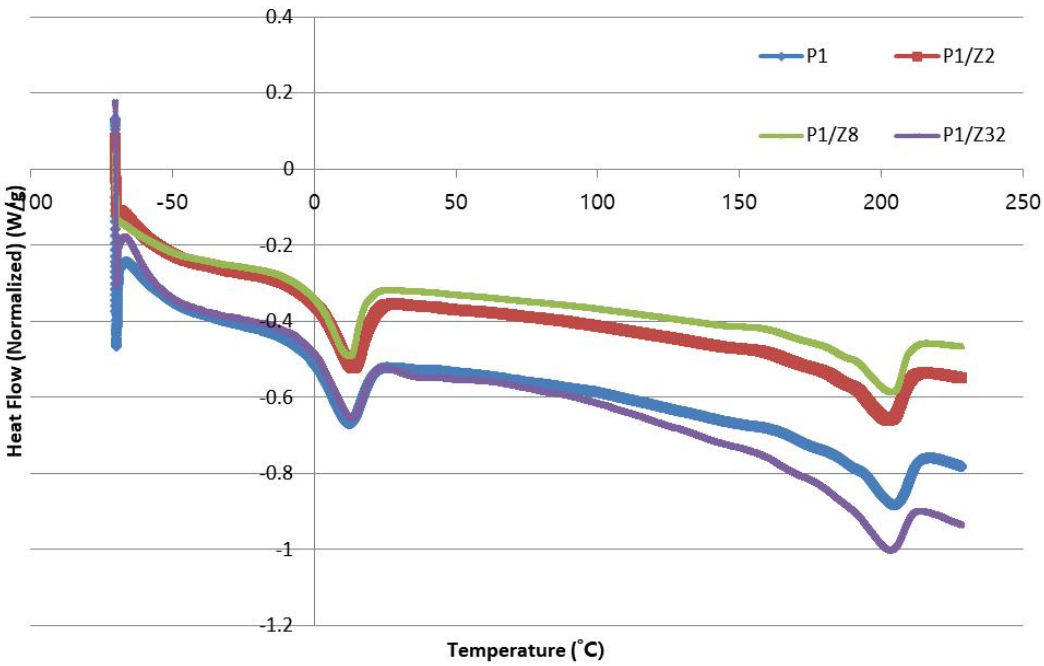

Figure 14 DSC curves of Pure Pebax 1657 and Pebax 1657/ZIF-8 MMM with different 2-MeIM/Zn

In Figure 15, exothermic peaks for PE segment and PA segment were observed as 11.044 ˚C (Figure A8) and 135.686 ˚C (Figure A8) for pure Pebax 2533. These exothermic peaks were similar to melting point of PE and PA in Pebax 2533, which are 9 ˚C (Table 5) and 126 ˚C (Table 1). Like Pebax 1657, adding different molar ratio of ZIF-8 into Pebax 2533 did not change peaks insignificantly. However, the enthalpy of PA in Pebax 2533 increased the most in P2/Z32 from

4.5115 (Figure A8) to 6.5797 J/g (Figure A11). This means that P2/Z32 has the highest crystallinity, which agrees with the XRD pattern of Pebax 2533/ZIF-8 and the peaks of the PA segment (Figure 13).

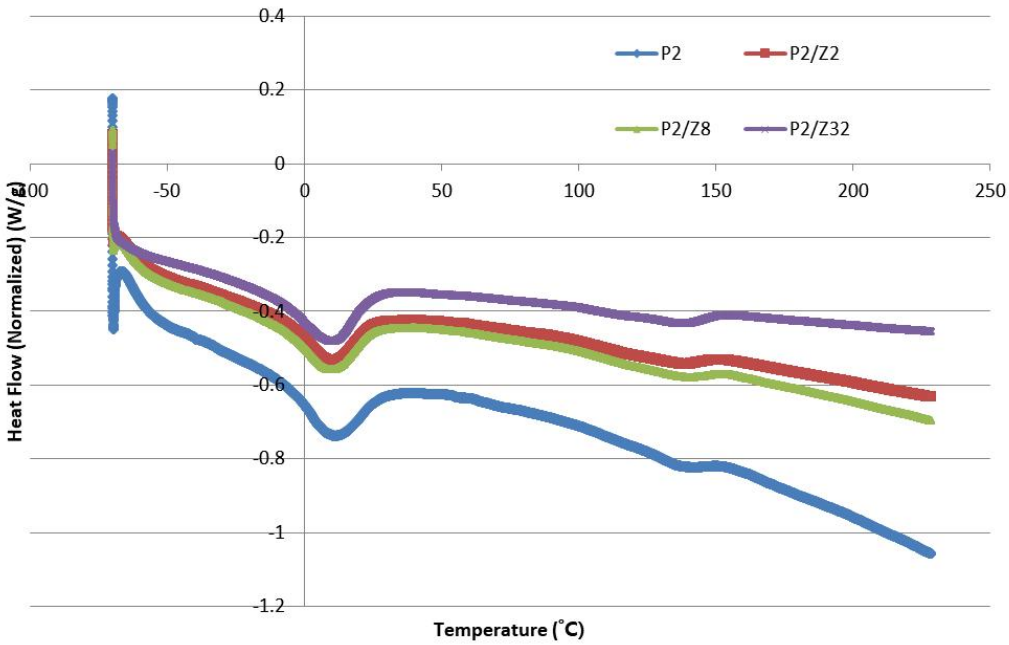

Figure 15 DSC curves of Pure Pebax 2533 and Pebax 2533/ZIF-8 MMM with 2-MeIM/Zn

The polymer crystallinity can be determined by measuring the enthalpy of fusion of the polymer (Sutrisna et al., 2017; Ghadimi et al., 2014) (Eq. (5)):

$$X_c = \frac{\Delta H_m}{\Delta H^\circ_m} \qquad (5)$$

where ΔH_m is the melting enthalpy of a semi-crystalline polymer and ΔH°_m is the melting enthalpy of the pure crystalline of PE and PA. The melting enthalpy of

PEO, PTMEO, and PA were 166.4, 200, and 230 J/g, respectively, which were obtained from literature (Sutrisna et al., 2017; Ghadimi et al., 2014; Bowman et al., 1969). The membrane crystallinity of PE and PA segments of Pebax/ZIF-8 MMMs was calculated (Table 3). The crystallinity in Pebax 1657 MMMs was lowest in P1/Z32. On the other hand, the crystallinity in Pebax 2533 MMMs was lowest in P2/Z2. Both DSC results of Pebax/ZIF-8 MMMs were in good agreement with XRD results.

Table 3 The degree of crystallinity of Pebax and Pebax/ZIF-8 MMMs based on DSC results

	$\triangle H_m$ (PE) (J/g)	$\triangle H_m$ (PA) (J/g)	X_{PE} (%)	X_{PA} (%)	Xc
P1	17.70	17.69	10.64	7.70	9.5
P1/Z2	17.35	17.38	10.43	7.56	9.3
P1/Z8	16.80	16.71	10.09	7.27	9.0
P1/Z32	13.09	17.19	7.87	7.47	7.7
P2	31.37	4.51	15.68	1.96	12.9
P2/Z2	27.48	5.48	13.74	2.38	11.5
P2/Z8	28.73	5.24	14.36	2.28	11.9
P2/Z32	29.94	6.58	14.97	2.86	12.5

The TGA graph shows the rate of change in weight of pure Pebax and Pebax/ZIF-8 MMM as a function of temperature. The weight change resulted from the decomposition of the Pebax and ZIF-8 structures. For Pebax 1657, decomposition temperature ranged between 300 ˚C and 450 ˚C, which agrees to previous work by Zheng et al. (2018). The TGA curves for both Pebax 1657/ZIF-8 MMM (Figure 16) and Pebax 2533/ZIF-8 MMM (Figure 17) have a first stage where water evaporates and second stage of weight loss from the Pebax MMM.

For pure Pebax 1657, 79.69% (Figure A12) was decomposed at 419.37 ˚C (Figure A12). For Pebax 1657/ZIF-8 MMM, 88.47% at 419.74 ˚C, 88.96% at 415.84 ˚C, and 88.45% at 415.58 ˚C were decomposed in P1/Z2, P1/Z8, and P1/Z32, respectively (Figure A13, A14, and A15). The decomposition temperature was lower in order of P1/Z32, P1/Z8, and P1/Z2. The DSC results of Pebax 1657/ZIF-8 show that enthalpy of PE of P1/Z32 was lower than that of P1/Z2 and P1/Z8. Therefore, the decomposition temperature of P1/Z32 was lowest. The decomposition temperatures of P1/Z2, P1/Z8, and P1/Z32 were lower than that of pure Pebax 1657 because of the oxidation of zinc in ZIF-8 particles. The zinc molecules in zinc nitrate hexahydrate catalyze the oxidation of Pebax 1657 and imidazolium ions in 2-methylimidazole (Jomekian et al., 2017).

For pure Pebax 2533, 98.50% was decomposed at 406.01 ˚C (Figure A16). For Pebax 2533/ZIF-8 MMMs, 94.17% at 430.57 ˚C, 94.14% at 429.66 ˚C, and 95.82% at 433.91 ˚C were decomposed in P2/Z2, P2/Z8, P2/Z32, respectively (Figure A17, A18, and A19). Unlike Pebax 1657, the decomposition temperatures of P2/Z2, P2/Z8, and P2/Z32 were higher than that of pure Pebax 2533. This results show similar trend from work of Nafisi et al. (2014), which decomposition temperature of Pebax 2533 was 350 ˚C, but it was increased up to 380 ˚C after adding ZIF-8 (Nafisi and Hagg, 2014).

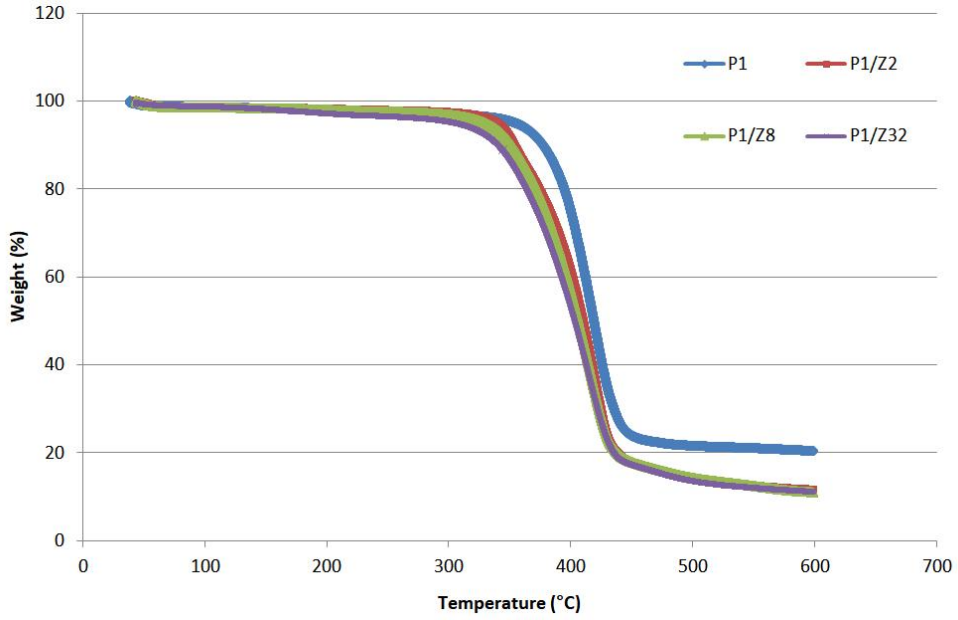

Figure 16 TGA curves of Pure Pebax 1657 and Pebax 1657/ZIF-8 MMM with different 2-MeIM/Zn

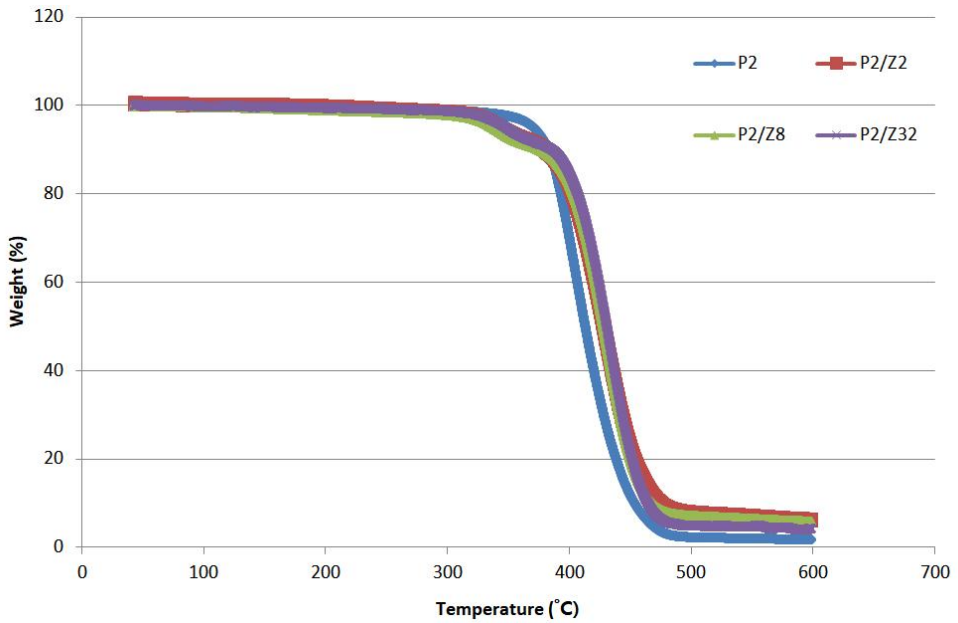

Figure 17 TGA curves of Pure Pebax 2533 and Pebax 2533/ZIF-8 MMMs with different 2-MeIM/Zn

3.3. The effect of controlling molar ratio of ZIF-8 on gas permeability of Pebax/ZIF-8 MMMs

3.3.1 The comparison of CO_2 permeability between Pebax 1657 and Pebax 2533

Figure 18 and 19 shows that the CO_2 permeability of Pebax 2533 MMMs was much higher than that of Pebax 1657 MMMs at the same temperature. The different CO_2 permeabilities can be explained by the chemical structure and affinity with CO_2 gas molecules. Bondar et al. (2000) and Kim et al. (2001) explained the difference in permeability of the two types of Pebax in terms of chemical structure, diffusivity, polarity, and solubility of Pebax. The chemical structure of Pebax 2533 has a higher content of rubbery PEO, which is a gas-transport-dominating phase, so it has higher permeability than Pebax 1657. The diffusivity of Pebax 1657 is lower than that of Pebax 2533 because it has more concentrations of polar groups in polymer matrix, which lowers gas diffusion coefficient (Bondar et al., 2000). However, the diffusivity of Pebax 1657 is lower for nonpolar gases such as N_2, but the solubility is higher for polar gases like CO_2. Therefore, the selectivity of CO_2/N_2 may be higher than that of Pebax 2533.

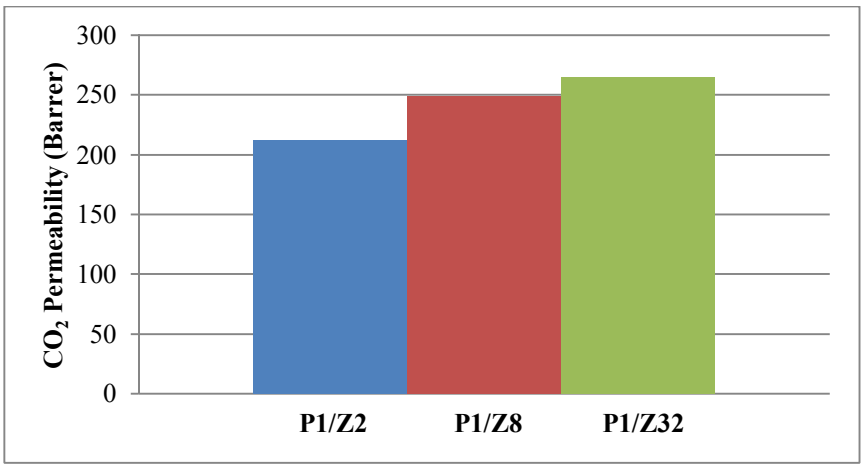

Figure 18 CO_2 permeability of Pebax 1657 MMMs with increasing molar ratio of ZIF-8 at 15 °C

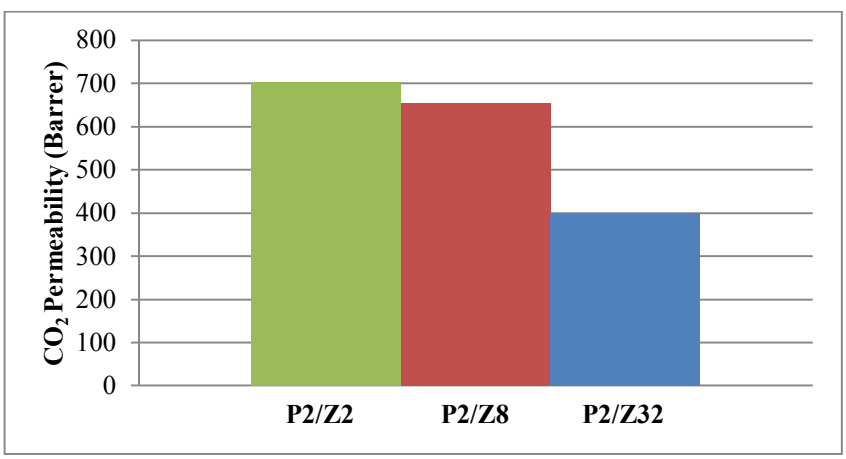

Figure 19 CO_2 permeability of Pebax 2533 MMMs with decreasing molar ratio of ZIF-8 at 15 °C

3.3.2 The comparison of CO_2 permeability between pure Pebax and Pebax/ZIF-8 MMMs

The permeability of pure Pebax 1657 was 83.7 barrer at 25 ˚C and 130 barrer at 40 ˚C, whereas the lowest permeability of P1/Z2 was 212 barrer at 15 ˚C (Figure 20). The permeability of pure Pebax 2533 was 272 barrer at 25 ˚C and 370 barrer at 40 ˚C, whereas the lowest permeability of P2/Z32 was 399 barrer at 15 ˚C (Figure 21). Therefore, the CO_2 permeability of Pebax/ZIF-8 MMM was higher than those of both Pebax 1657 and Pebax 2533 alone, even at much lower temperature.

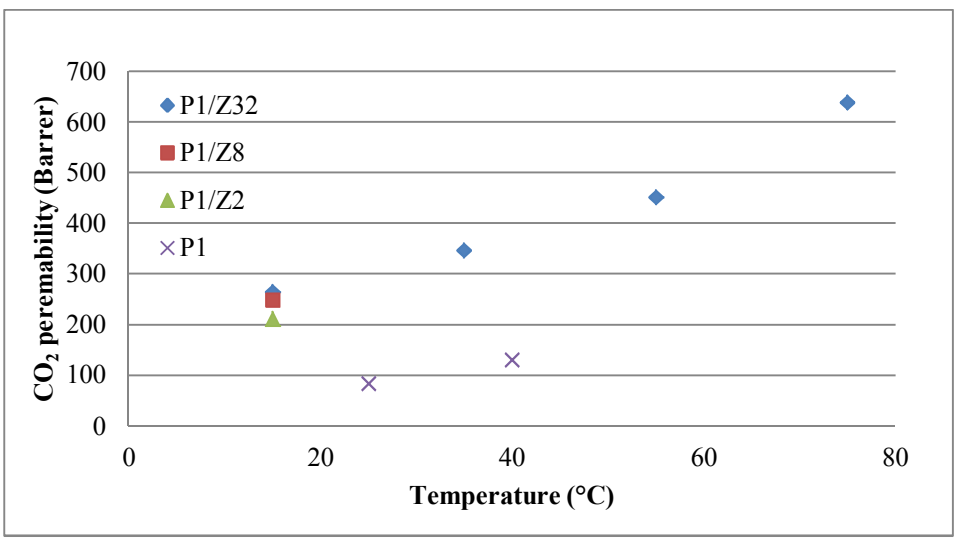

Figure 20 CO_2 permeability of P1, P1/Z2, P1/Z8, and P1/Z32 with increasing temperature

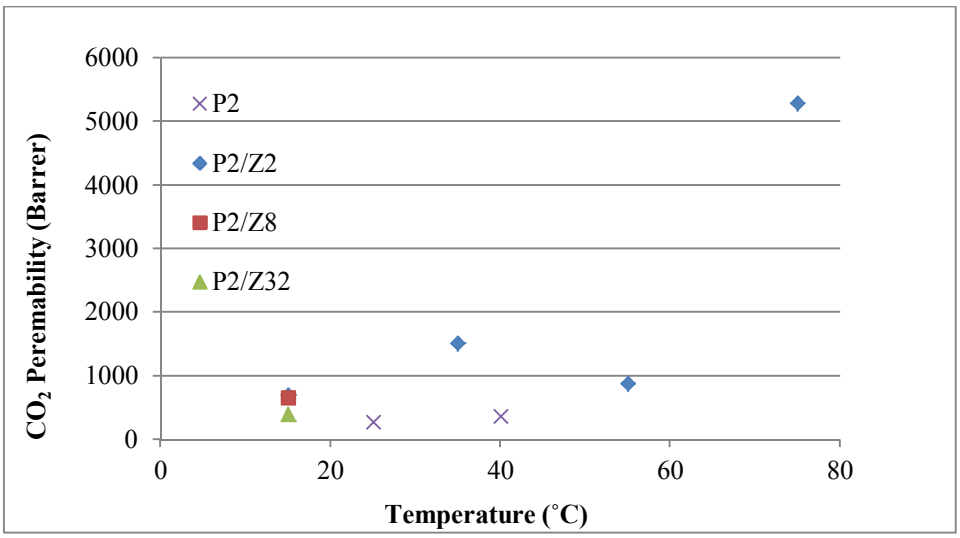

Figure 21 CO_2 permeability of P2, P2/Z2, P2/Z8, and P2/Z32 with increasing temperature

The higher CO_2 permeability of Pebax with the incorporation of ZIF-8 particles can be achieved by high CO_2 diffusivity and solubility of ZIF-8 (Xu et al., 2017; Sutrisna et al., 2017). Flexible porous structures of ZIF-8 increase free volume in Pebax matrix, which can improve diffusion of gas molecules with large kinetic diameters (Song et al., 2012). Free volume in polymer refers to the free room where polymer chains may move and occupy in polymer (Choudalakis and Gotsis, 2012). When nanoparticles are embedded in polymer matrix, large surface areas of nanoparticle create interfacial regions which are connected by weak interaction between inorganic particle and organic polymer (Choudalakis and Gotsis, 2012). Furthermore, at the interfacial region between ZIF-8 and Pebax, ZIF-8 particles form hydrogen bonding with PA in Pebax, which occur between (1) the aldehyde groups in the PA segment and methyl groups in the 2-methylimidazole in the ZIF-8, as well as (2) N-H groups in the PA and N atoms of the imidazole ring (Mahdi et al., 2016). ZIF-8 particles not only enhance structural

stability by forming hydrogen bonds with PA (Sutrisna et al., 2017), but also disrupt chain packing of PEO segment in Pebax (Sutrisna et al., 2017). Therefore, the PEO chain interaction is decreased, resulting in increasing free volume for penetrants to diffuse (Sutrisna et al., 2017). Also, CO_2 adsorption capacity in ZIF-8 is high since polar organic ligands of 2-MeIM in ZIF-8 adsorb polar CO_2 molecule selectively, which can improve CO_2 solubility (Xu et al., 2016; Jomekian et al. 2016; Sutrisna et al., 2017).

Therefore, the enhancement of the free volume is a mechanism for increasing diffusion, which is described by the Cohen and Turnbull equation (Eq. (6)):

$$D = A\, exp\left(\frac{-\gamma V^*}{V_f}\right) \qquad (6)$$

where D is the diffusion coefficient, A is the pre-exponential factor, γ is an overlap factor to avoid the double-counting of free volume elements, V^* is the minimum free volume elementsize that a penetrant can pass, and V_f is the average free volume in the polymer that is available for a penetrant to be transported through (Cong et al., 2006). Therefore, incorporation of ZIF-8 on Pebax increases both diffusivity and solubility, which can improve the permeability based on the solution-diffusion mechanism in Eq. (7):

$$P_i = D_i * S_i \qquad (7)$$

where P_i is the permeability of gas i, D_i is the average effective diffusion coefficient, and S_i is the solubility coefficient.

3.3.3 The comparison of CO_2 permeability between Pebax 1657 MMMs and Pebax 2533 MMMs in terms of ZIF-8 with different molar ratio

The effect of increasing molar ratios of ZIF-8 precursors on the CO_2 permeability was investigated (Figure 18-21). At a temperature of 15 ˚C, Pebax 1657/ZIF-8 MMM showed the highest CO_2 permeability with P1/Z32, followed by P1/Z8 and P1/Z2. At the same temperature, Pebax 2533/ZIF-8 MMM showed the highest CO_2 permeability for P2/Z2, followed by P2/Z8 and P2/Z32.

There are several important factors in the opposite trends of CO_2 permeability for Pebax 1657/ZIF-8 and Pebax 2533/ZIF-8 based on different molar ratios of ZIF-8 precursors (Figure 20 and 21): (1) particle size, numbers of pore, and pore size of ZIF-8 with increasing molar ratio of 2-MeIM/Zn, (2) the polarity of Pebax, (3) the affinity for CO_2 gas molecules, and (4) the crystallinity change of Pebax MMMs in terms of ZIF-8 molar ratio.

For Pebax 1657 MMMs, as the molar ratio 2-MeIM/Zn of ZIF-8 precursors increased, the CO_2 permeability at a fixed temperature of 15 ˚C increased (Figure 20). Jomekian et al. (2016) reported on the trend of increasing permeability of Pebax 1657/ZIF-8 corresponding to increasing molar ratios of 2-MeIM/Zn. The increasing molar ratio of 2-MeIM/Zn increases the CO_2 permeability by higher gas sorption capacity (Jomekian et al., 2016). Increasing molar ratio of 2-MeIM/Zn showed higher BET surface area (Jomekian et al., 2016). As the sizes of nanoparticles decrease, the surface areas become larger and create interfacial regions in the organic polymers (Pleşa et al., 2016).

The polarity of Pebax is another important factor of the permeability increase of Pebax 1657 MMMs with increasing molar ratio 2-MeIM/Zn of ZIF-8. Pebax

1657 has a high concentration of polar groups in PEO chain segments, which have a high affinity for CO_2 (Bondar et al., 2000). Imidazolium ions and PEO segments in the Pebax 1657 result in excessive adsorption of CO_2 molecules (Jomekian et al., 2016). Excessive sorption of CO_2 by imidazolium ions causes plasticization of Pebax 1657, which enhances the polymer chain mobility (Jomekian et al., 2016). The result of highest permeability of Pebax 1657 with increasing 2-MeIM/Zn can be also explained by the crystallinity change with incorporation of ZIF-8 with increasing 2-MeIM/Zn. P1/Z32 showed the lowest crystallinity in DSC results (Table 3), which showed the highest CO_2 permeability.

However, for Pebax 2533 MMMs, increasing the molar ratio of ZIF-8 resulted in lower CO_2 permeability at 15 ˚C (Figure 21). When the molar ratio of 2-MeIM/Zn increases, the shape of ZIF-8 particles changes from cubical to spherical (Figure 3), and as a result, the fillers aggregate and tend to fill the interstitial regions of the polymer, which could prevent access to the polymer matrix (Choudalakis et al., 2012). As the molar ratio of 2-MeIM/Zn increased, ZIF-8 particles form more hydrogen bonding with PA in Pebax 2533, which may lead weaker polymer chain packing of PTMEO (Sutrisna et al., 2017; Ghadimi et al., 2014). The diffusivity may be decreased by the smaller pore size and particle size of ZIF-8 with increasing molar ratio of 2-MeIM/Zn. According to Jomekian et al. (2016) increasing the ZIF-8 molar ratio decreases the particle size and pore volume of ZIF-8 particles. As molar ratio of ZIF-8 increases, the particle size of ZIF-8 decreases along with the pore size (Jomekian et al., 2016). This implied that particles aggregate more and may reduce space in the polymer matrix for penetrants to diffuse.

Compared to Pebax 1657, the polarity of Pebax 2533 is lower in the PTMEO segment, which has a low affinity for CO_2 (Bondar et al., 2000). When the molar ratio of 2-MeIM/Zn is increased, the concentration of polar imidazolium ions in

ZIF-8 is increased. However, less polar PTMEO in Pebax 2533 may not be enough to interact with imidazolium to adsorb CO_2 and enhance the polymer chain mobility. It suggested that increasing the molar ratio of ZIF-8 could prevent the interstitial volume from accessing the polymer segment and decreased the free volume and diffusivity. Although the loading ZIF-8 of any molar ratio in Pebax 2533 enhanced the permeability of CO_2 molecules compared to pure Pebax 2533, increasing the molar ratio was not effective for Pebax 2533 to enhance the CO_2 permeability. The result of highest CO_2 permeability of Pebax 2533 with decreasing 2-MeIM/Zn can be also explained by the lowest crystallinity of P2/Z2 in DSC results (Table 3).

In the XRD, DSC, and TGA results, the Pebax 1657 MMM showed the lowest crystallinity with Z32, and Pebax 2533 MMM showed the lowest crystallinity with Z2. Kim et al. (2001) reported that the crystallinity region in a Pebax polymeric matrix decreases the permeability of the Pebax because the crystalline phase forms uniform and rigid chains that lack sorption sites and the mobility of chains for the permeation of penetrants. Therefore, Pebax 1657 is more effective for the permeation of CO_2 with Z32, whereas Pebax 2533 is more effective for the permeation of CO_2 with Z2.

3.4. The effect of temperature on gas permeability of Pebax/ZIF-8 MMMs with different molar ratio of ZIF-8

To confirm the effect of the permeating temperature on Pebax MMMs, the MMMs with the highest permeabilities were tested with CO_2 gas and N_2 gas at increasing temperature. Pebax 1657/ZIF-8 MMM with a molar ratio of 32/1 and Pebax 2533/ZIF-8 with molar ratio of 2/1 were used at a constant feed pressure of 3 bar and temperatures of 15, 35, 55, and 75 ˚C (Figure 20 and 21). As the temperature increased, the CO_2 permeability obtained with both P1/Z32 and P2/Z2 increased.

The temperature dependency of the permeability was calculated using the van't Hoff-Arrhenius equation (Eq. (8)):

$$P = P_o \, exp\left(-\frac{E_P}{RT}\right), \; E_p = E_d + \Delta H_s \qquad (8)$$

where P is the permeability coefficient, P_0 is a pre-exponential factor, and E_P is the activation energy of permeation, which is the sum of the activation energy for diffusion, E_d, and the enthalpy of sorption, ΔH_s (Kim et al., 2001; Cong et al., 2007). R is gas constant, and T is operating temperature (Acharya and Yadav, 2004). According to Eq. (8), if either the activation energy for diffusion or the enthalpy of sorption decreases, the permeability increases.

According to Kim et al. (2001), the enthalpy of sorption of CO_2 is negative, whereas that of N_2 is positive (Table 4). A smaller enthalpy of CO_2 sorption mainly results from the condensable and polarizable tendencies of CO_2 toward the polymer chain. Furthermore, increasing the temperature from below the melting point (T_m) to above T_m of Pebax 1657 resulted in more of a decrease of the activation energy of permeation (Table 4), because increased segmental motion of gas molecules in

the polymer matrix decreases the activation energy of diffusion. Furthermore, highly polar imidazolium ions are able to adsorb more CO_2 molecules, resulting in lower enthalpy for the sorption of CO_2, which increases CO_2 permeability.

Table 4 The activation energies of permeation and diffusion, and heat of sorption (kJ/mol) for CO_2 and N_2 gases below and above the melting point (T_m) of Pebax 1657 (Kim et al., 2001)

		E_p	E_d	ΔH_s
Below T_m	CO_2	14.6	27.2	-12.6
	N_2	33.6	29.7	3.93
Above T_m	CO_2	10.9	25.7	-14.8
	N_2	26.2	24.3	1.90

A logarithmic function was applied to the van't Hoff-Arrhenius equation to calculate the pre-exponential factor P_o and activation energy of permeation, E_p (Figure 22 and 23) from following Eq. (9):

$$log\ P = -\frac{E_p}{R} \cdot \frac{1}{T} + log\ P_o \qquad (9)$$

The activation energy of permeation can be calculated from the slope of the log of permeability, $-\frac{E_p}{R}$. Before filling the Pebax polymer with ZIF-8, the activation energy of permeation of Pebax 2533 is lower than that of Pebax 1657 (Table 5). The enthalpy of sorption of pure Pebax 1657 (-13.4 kJ/mol) is lower than that of pure Pebax 2533 (-10.5 kJ/mol), but the activation energy of diffusion of Pebax 1657 (32 kJ/mol) is higher than that of Pebax 2533 (27.2 kJ/mol) (Table 5)

(Rahman et al., 2013). The resulting activation energy of permeation of Pebax 2533 is 16.7 kJ/mol, which is lower than that of Pebax 1657 (18.6 kJ/mol). Therefore, Pebax 2533 has higher permeability than Pebax 1657 (Rahman et al., 2013). However, after adding ZIF-8 particles into the Pebax polymer, the activation energy of permeation of P1/Z32 (5.2 x 10^{-3} kJ/mol) was lower than that of P2/Z2 (9.7 x 10^{-3} kJ/mol). The polar groups of Pebax 1657 interact with highly polar imidazolium ions in ZIF-8 nanoparticles and adsorb more CO_2 molecules by plasticization. This decreases the enthalpy of sorption, resulting in lower activation energy of permeation.

Table 5 Important chemical properties of Pebax 1657 and Pebax 2533 related to gas permeability

Polymer type	Pebax 1657	Pebax 2533	Ref.
T_g (˚C)	-51.7	-77	Zheng et al. Mohr et al.
T_m (˚C)	50	9	Kim et al. Mohr et al.
E_p (kJ/mol)	18.6	16.7	Rahman et al.
E_d (kJ/mol)	32	27.2	Rahman et al.
$\triangle H_s$ (kJ/mol)	-13.4	-10.5	Rahman et al.

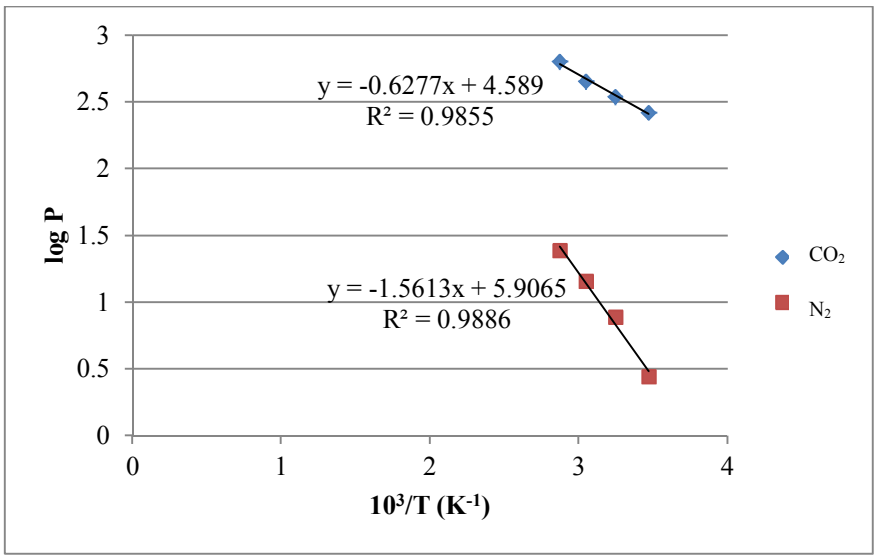

Figure 22 The correlation of permeability and temperature with preexponential constant (P_o) and activation energy of permeation (E_p) of P1/Z32

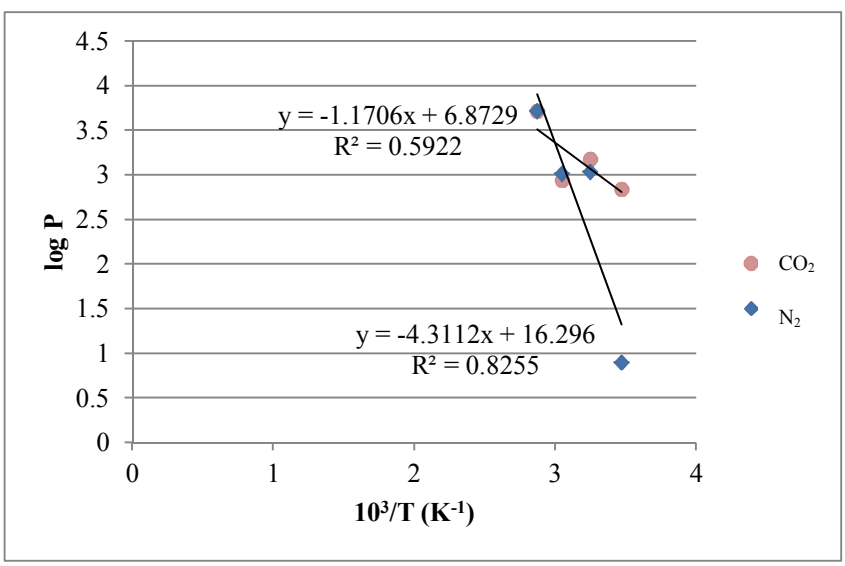

Figure 23 The correlation of permeability and temperature with preexponential constant (Po) and activation energy of permeation (E_p) of P2/Z2

From Eq. (9), the pre-exponential factor P_o can be calculated by 10 to the power of the y-intercept. The pre-exponential factor and activation energy of permeation are high when penetrants are not significantly affected by the temperature change (Chen and Feng, 2004). According to Table 6, both the activation energy of permeation and pre-exponential factor of Pebax 1657 were lower than those of Pebax 2533, which means that Pebax 1657 MMM is more sensitive to temperature changes, and the permeability was increased more significantly, even though the increase of temperature increases the permeability for both Pebax 1657 MMM and Pebax 2533 MMM. When the temperature increases, the interaction between more polar PEO groups in Pebax 1657 and polar imidazolium ion in ZIF-8 may affect the permeability of penetrants. The reason is that the enthalpy of sorption is decreased by the plasticization of polar groups in the polymeric matrix. On the other hand, less polar PTEMO groups in Pebax 2533 are less polarizable to adsorb CO_2, which may result in less of a decrease in the enthalpy of sorption than Pebax 1657 MMM.

Table 6 Activation energy of permeation and preexponential factor of Pebax 1657/ZIF-8 32/1M and Pebax 2533/ZIF-8 2/1M

MMMs	Penetrant Gas	E_p (kJ/mol)	P_o (Barrer)
Pebax 1657	CO_2	5.2×10^{-3}	3.88×10^{4}
ZIF-8 32/1M	N_2	1.3×10^{-2}	8.06×10^{5}
Pebax 2533	CO_2	9.7×10^{-3}	7.46×10^{6}
ZIF-8 2/1M	N_2	3.5×10^{-2}	1.98×10^{16}

As the permeating temperature increased, the selectivity of CO_2/N_2 decreased for both P1/Z32 and P2/Z2 (Figure 24 and 25). This phenomenon occurred for both Pebax/ZIF-8 and pure Pebax. Kim et al. (2001) reported that the CO_2/N_2 selectivity of Pebax 1657 at 3 atm decreased from 71 at 25 ˚C to 47 at 45 ˚C, 29 at 65 ˚C, and 20 at 85 ˚C. As the temperature increases, the polymer loses its chemical nature of favoring particular gases because segmental motion of the gas molecules increases regardless of the penetrants (Chen and Feng, 2004). Also, Bondar et al. (2000) explained that selectivity of CO_2/nonpolar gases like N_2 is lower for PTMEO/PA12 copolymers like Pebax 2533, because they have less polar ether linkages to adsorb CO_2 than PEO/PA6 copolymers like Pebax 1657. Furthermore, Bondar et al. (2000) explained that the selectivity of CO_2/nonpolar gases like N_2 is lower for PTMEO/PA12 copolymers like Pebax 2533 because they have less polar ether linkages to adsorb CO_2 than PEO/PA6 copolymers like Pebax 1657. Furthermore, Pebax 2533 has a higher concentration of PTMEO (a transport-dominating phase) than the concentration of PEO in Pebax 1657, which enhances the diffusivity. Therefore, based on Figure 23 and 24, Pebax 2533 has higher permeability than Pebax 1657, but Pebax 1657 is much more efficient for the selectivity of CO_2/N_2.

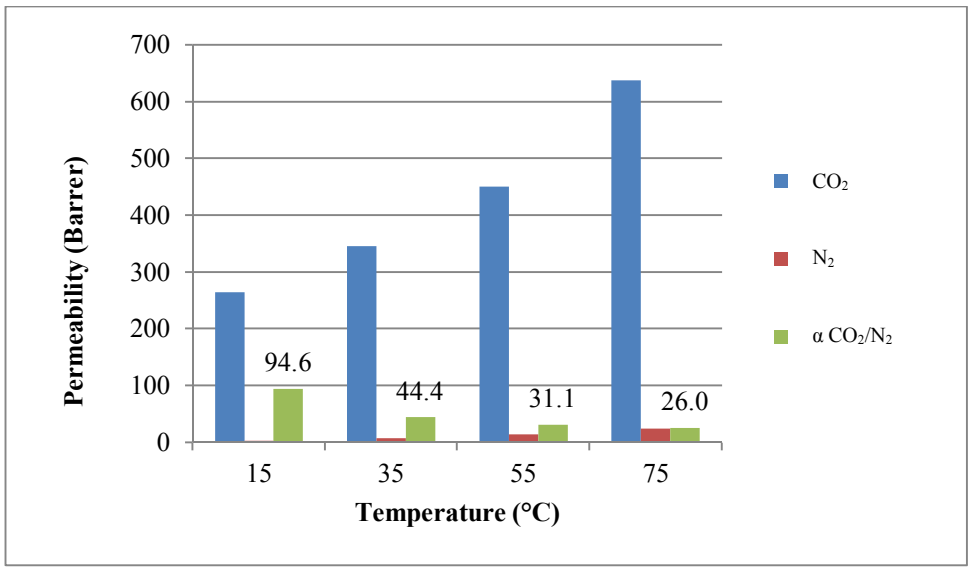

Figure 24 Single CO_2 and N_2 gas permeability and selectivity of P1/Z32 with increasing temperature

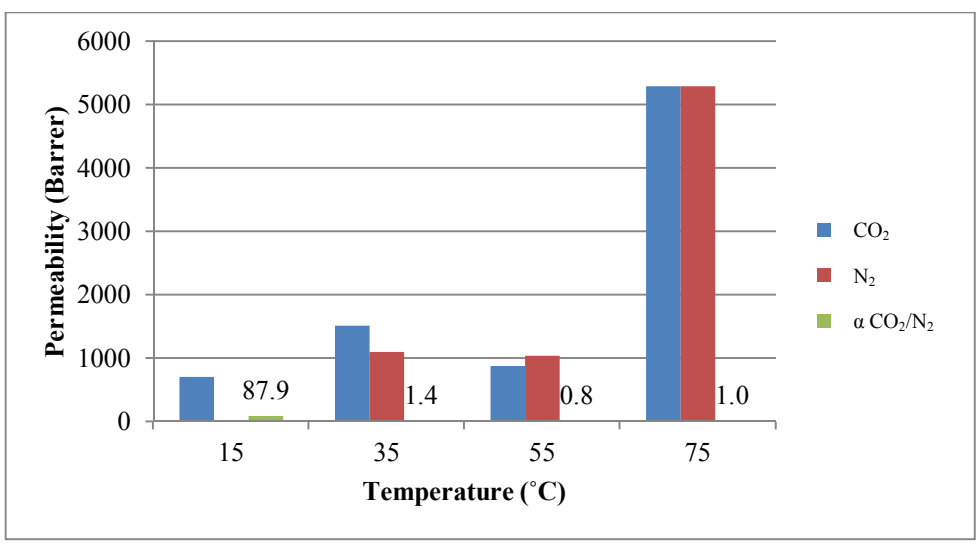

Figure 25 Single CO_2 and N_2 gas permeability and selectivity of P2/Z2 with increasing temperature

For both Pebax 1657 and 2533, the permeabilities were significantly higher after using the ZIF-8 filler and increasing the permeating temperature. The ZIF-8 filler increased the CO_2 solubility of Pebax 1657 more than that of Pebax 2533 through plasticization of the polar groups. Increasing the permeating temperature increased the permeabilities of both Pebax 1657/ZIF-8 and Pebax 2533/ZIF-8. However, the permeability of Pebax 1657/ZIF-8 MMM was more dependent on the temperature, which was proven by the low activation energy of permeation and enthalpy of sorption. Therefore, Pebax 1657 was more suitable for increasing the CO_2/N_2 selectivity through interactions with polar imidazolium ions at a molar ratio 32/1 of ZIF-8. On the other hand, Pebax 2533 was more suitable for increasing the CO_2 permeability through increasing the fractional free volume of the polymeric matrix by adding less aggregating ZIF-8 with a molar ratio of 2/1.

Chapter 4. Conclusion

In this study, the effect of 2-MeIM/Zn molar ratio of ZIF-8 on the performance of CO_2 and N_2 permeation of Pebax 1657 and Pebax 2533 MMMs was investigated. The studies of CO_2 permeability of Pebax 1657/ZIF-8 MMMs with controlling molar ratio of ZIF-8 has been reported by previous research. However, CO_2 permeability of Pebax 2533/ZIF-8 MMMs with controlling molar ratio was investigated in this work, which was explained by important relationship between ZIF-8 and Pebax based on their chemical structures and morphological characteristics that determine the CO_2 permeability. ZIF-8 with a higher molar ratio of 2-MeIM/Zn had smaller size and showed weaker and wider peaks than that of ZIF-8 with a lower molar ratio of 2-MeIM/Zn, which represents the chemical nature of an amorphous material.

The CO_2 and N_2 permeability were higher in Pebax/ZIF-8 MMMs than in pure Pebax. In terms of different molar ratio of ZIF-8, the CO_2 and N_2 permeability were highest for Pebax 1657 MMM with ZIF-8 molar ratio of 32/1 and for Pebax 2533 MMM with ZIF-8 molar ratio of 2/1. Since Pebax 1657 has polar PE segment (60% of PEO), higher sorption capacity of ZIF-8 molar ratio of 32/1 enhanced CO_2 sorption, which resulted in improvement of CO_2 selectivity over N_2. On the other hand, since Pebax 2533 has higher PE content (80% of PTMEO), but has lower polarity, which provides higher gas transport, less aggregating ZIF-8 particles with molar ratio of 2/1 enhanced free volume of Pebax 2533, which resulted in increase of CO_2 permeability.

The effect of temperature on the CO_2 and N_2 permeability was investigated as well. As the temperature increased, the permeabilities both increased for Pebax 1657/ZIF-8 and Pebax 2533/ZIF-8 MMMs. As the temperature increases, the

diffusivity of polymer increased for all gas molecules, so the CO_2/N_2 selectivity decreased for both Pebax 1657 and 2533. Also, the porous structure of ZIF-8 increased the micro-void in Pebax matrix, which increased the free volume for diffusion of all gas molecules.

In summary, Pebax 1657/ZIF-8 with a molar ratio of 32/1 and Pebax 2533/ZIF-8 with a molar ratio of 2/1 had the best performance for CO_2 permeation. This means that better permeability and compatibility between the polymer and particles can be achieved by controlling the molar ratio of ZIF-8 precursors and selecting the right Pebax polymer based on the chemical nature and interfacial interactions. The CO_2/N_2 selectivity of Pebax 1657 MMMs with ZIF-8 molar ratio of 2/1 and 8/1 and that of Pebax 2533 MMMs with ZIF-8 molar ratio of 8/1 and 32/1 may be investigated for finding optimal conditions for the CO_2/N_2 selectivity of Pebax /ZIF-8 MMMs with ZIF-8 molar ratio.

References

Acharya, N. K. and Yadav, P. K., 2004, Study of temperature dependent gas permeability for polycarbonate membrane, *Indian Journal of Pure & Applied Physics*, **42**, 179-181.

Balzar, D. and Audebrand, N., Daymond, M. R., Fitch, A., Hewat, A., Langford, J. I., Le Bail, A., Loue¨r, D., Masson, O., McCowan, C. N., Popa, N. C., Stephens, P. W., Toby, B. H., 2004, Size-Strain Line-Broadening Analysis of the Ceria Round-Robin Sample, *Journal of Applied Crystallography*, **37**, 911-924.

Bondar, V. I., Freeman, B. D., Pinnau, I., 2000, Gas Transport Properties of Poly(ether-b-amide) Segmented Block Copolymers, *Journal of Polymer Science: Part B: Polymer Physics*, **38**, 2051-2062.

Bowman, I.J.W., Brown, D.S., Wetton, R.E., 1969, Crystal density, crystallinity and heat of fusion of poly (tetramethylene oxide), *J. Polym. Sci*. **10,** 715-718.

Chen, J. C. and Feng, X., 2004, Gas Permeation Through Poly(Ether-b-amide) (PEBAX 2533) Block Copolymer Membranes, *Separation Science and Technology*, **39** (1), 149-164.

Choudalakis, G. and Gotsis, A. D., 2012, Free volume and mass transport in polymer nanocomposites, *Current Opinion in Colloid & Interface Science*, **17**, 132-140.

Cohen, M. H. and Turnbull, D., 1959, Molecular transport in liquids and glasses, *J. Chem. Phys*. **31**, 1164-1169.

Cong, H., Radosz, M., Towler, B. F., Shen, Y., 2007, Polymer-inorganic nanocomposite membranes for gas separation, *Separation and Purification Technology,* **55**, 281-291.

Ghadimi, A., Amirilargani, M., Mohammadi, T., Kasiri, N., Sadatnia, B., 2014, Preparation of alloyed poly(ether block amide)/poly(ethylene glycol diacrylate) membranes for separation of CO_2/H_2 (syngas application), *J. Membr. Sci*. **458**, 14–26.

Hu, Q. and Marard, E., 1997, Poly(amide-imide)/TiO_2 nano-composite gas separation membranes: fabrication and characterization, *J. Membr. Sci*. **135**, 65-79.

Jian, M., 2015, Water-based synthesis of zeolitic imidazolate framework-8 with high morphology level at room temperature, *The Royal Society of Chemistry*, **5**, 48433-48441.

Jomekian, A. Bazooyar, B., Behbahni, M., Mohammadi, T., Kargari, A., 2017, Ionic liquid-modified Pebax 1657 membrane filled by ZIF-8 particles for separation of CO_2 from CH_4, N_2, and H_2, *J. Membr. Sci.*, **524**, 652-662.

Jomekian, A., Behbahani, R. M., Mohammadi, T., Kargari, A., 2016, Utilization of Pebax 1657 as structure directing agent in fabrication of ultra-porous ZIF-8, *Journal of Solid State Chemistry*, **235**, 212-216.

Jomekian, A., Behbahani, R.M., Mohammadi, T., Kargari, A., 2016, CO_2/CH_4 separation by high performance co-coasted ZIF-8/Pebax 1657/PES mixed matrix membrane, *Journal of Natural Gas Science and Engineering*, **31**, 562-574.

Kim, J. H. Ha, S.Y., Lee, Y. M., 2001, Gas permeation of poly(amide-6-b-ethylene oxide) copolymer, *J. Membr. Sci.*, **190**, 179-193.

Koros, W.J. and Lively, R.P., 2012, Water and beyond: expanding the spectrum of large-scale energy efficient separation processes, *AIChE J.*, **58** (9), 2624–2633.

Lin, H. and Freeman, B.D., 2005, Materials selection guidelines for membranes that remove CO_2 from gas mixtures, *J. Mol. Struct*., **739** 57-74.

Maier, G., 1998, Gas separation with polymer membranes, *Angew. Chem. Int. Ed.*, **37**, 2960-2974.

Mohr, J. M. and Paul, D. R., 1991, Gas transport properties of a series of poly(ether ketone) polymers, *Polymer*, **32** (13), 2387-2394.

Nafisi, V. and Hagg, M. B., 2014, Development of dual layer of ZIF-8/PEBAX-2533 mixed matrix membrane for CO_2 capture, *Journal of Membrane Science*, **459**, 244-255.

Okamoto, K.I., Fuji, M., Okamyo, S., Suzuki, H., Tanaka, K., Kita, H., 1995, Gas permeation properties of poly(ether imide) segmented copolymers, *Macromolecules*, **28**, 6950-6956.

Peng, F. and Lu, L., 2005, Hybrid organic-inorganic membrane: solving the trade-off between permeability and selectivity, *Chem. Mater*. **17,** 6790-6796.

Plesa, I., Notingher, P. V., Schlögl, S., Sumereder, C., Muhr, M., 2016, Properties of Polymer Composites Used in High-Voltage Applications, *Polymer*, **8**, 173.

Rabiee, H., Ghadimi, A., Mohammadi, T., 2015, Gas transport properties of reverse-selective poly(ether-b-amide6)/[Emim][BF4] gel membranes for CO_2/light gases separation, *J. Membr. Sci*., **476**, 286-302.

Rahman, M., Filiz, V., Shishatskiy, S., Abetz, C., Neumann, S., Bolmer, S., Khan, M. M., Abetz, V., 2013, PEBAX® with PEG functionalized POSS as nanocomposite membranes for CO_2 separation, *Journal of Membrane Science*, **437**, 286-297.

Rezakazemi, M., Amooghin, A.E., Montazer-Rahmati, M.M., Ismail, A. F., Matsuura, T., 2014, State-of-the-art membrane based CO_2, separation using mixed matrix membranes (MMMs): an overview on current status and future directions, *Prog. Polym. Sci.*, **39** (5), 817–861.

Robeson, L.M., 2008, The upper bound revisited, *J. Membr. Sci*., **320**, 390-400.

Shen, J., Liu, G., Huang, K., Li, Q., Guan, K., Li, Y., Jin, W., 2016, UiO-66-polyether block amide mixed matrix membranes for CO_2 separation, *J. Membr. Sci*., **513**, 155-165.

Sutrisna, P. D., Hou, J., Li, H., Zhang, Y., Chen, V., 2017, Improved operational stability of Pebax-based gas separation membranes with ZIF-8: a comparative study of flat sheet and composite hollow fibre membranes, *Journal of Membrane Science*, **524**, 266-279.

Xu, L., Xiang, L. Wang, C., Yu, J., Pan, Y., 2017, Enhanced permeation performance of polyether-polyamide block copolymer membranes through incorporating ZIF-8 nanocrystals, *Chinese Journal of Chemical Engineering*, **25,** 882-891.

Zhang, Y., Jia, Y., Li, M., Hou, L., 2018, Influence of the 2-methylimidazole/zinc nitrate hexahydrate molar ratio on the synthesis of zeolitic imidazolate framework-8 crystals at room temperature, *Scientific Reports*, **8**, 9597

Zheng, W. and Ding, R., 2018, ZIF-8 nanoparticles with tunable size for enhanced CO_2 capture of Pebax based MMMs, *Sep. Purif. Technol.*, **214**, 111-119.

Appendices

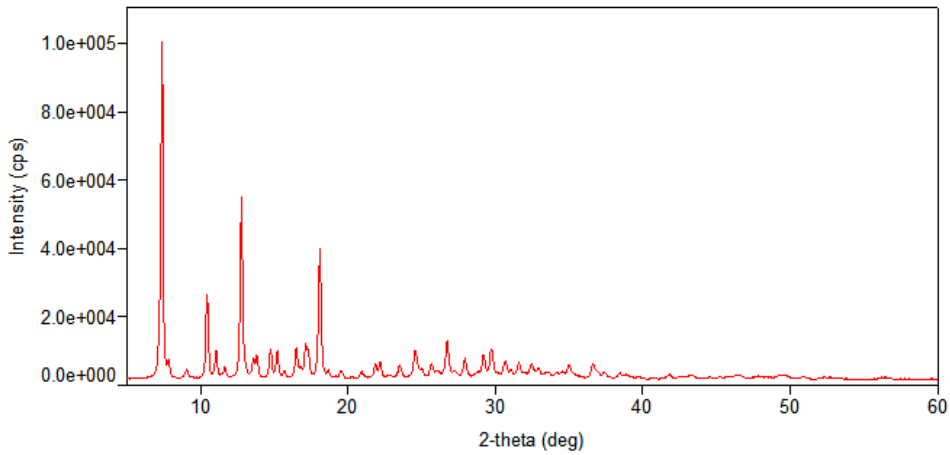

Figure A1 XRD graphs of Z2

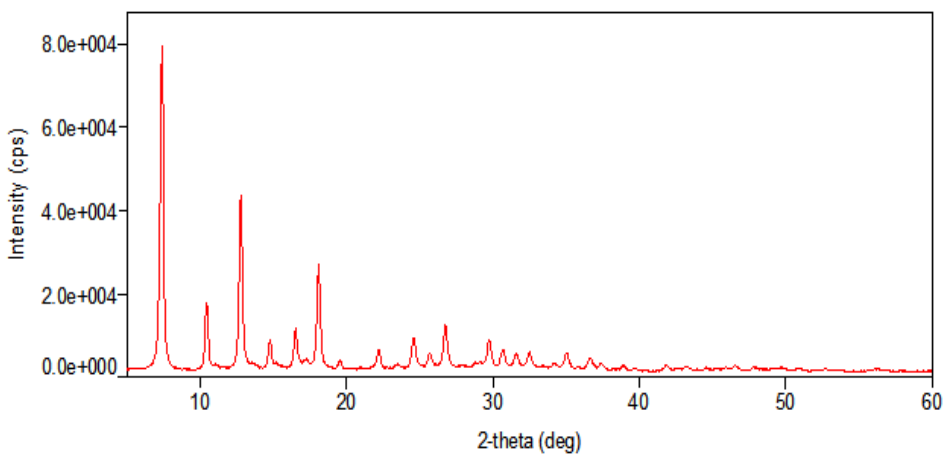

Figure A2 XRD graphs of Z8

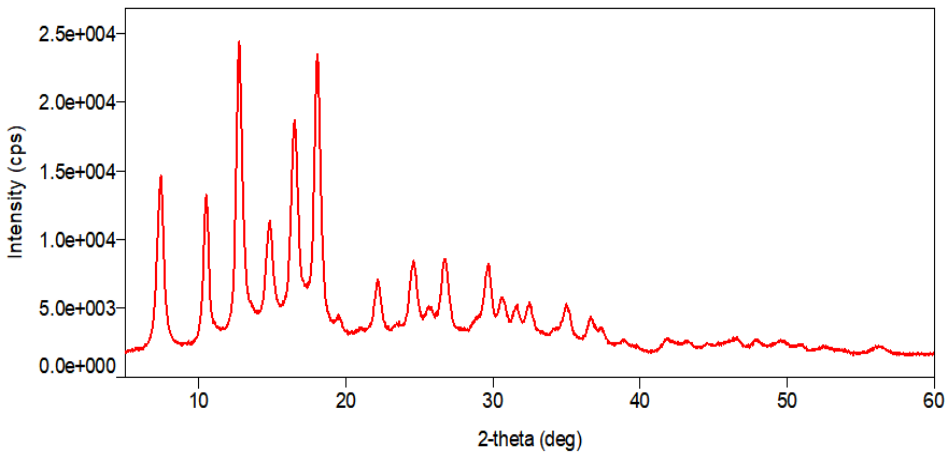

Figure A3 XRD graphs of Z32

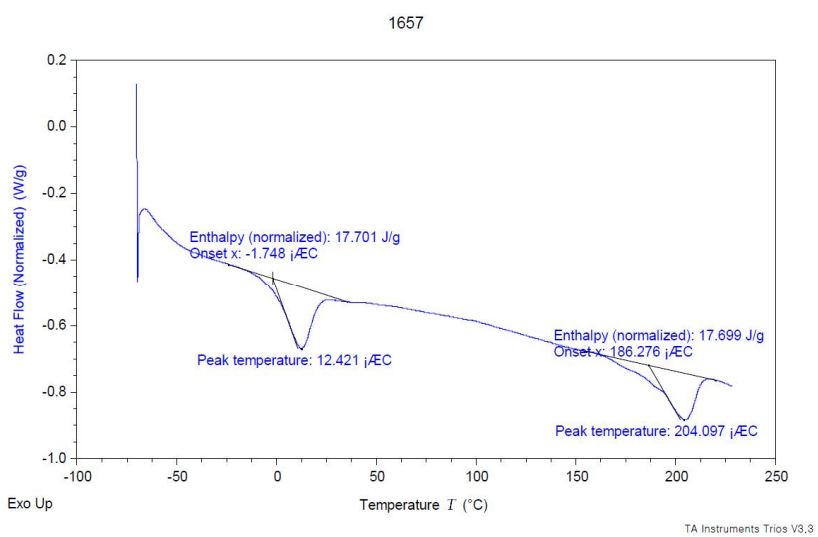

Figure A4 DSC curve of pure P1

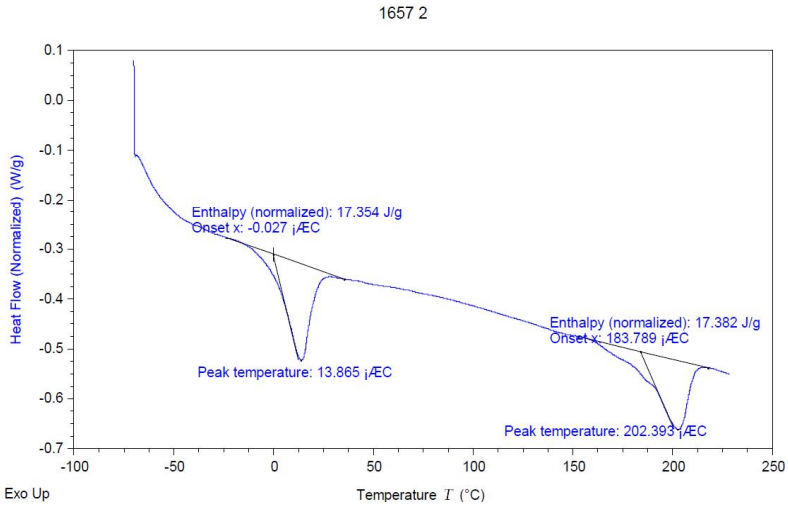

Figure A5 DSC curve of P1/Z2 MMM

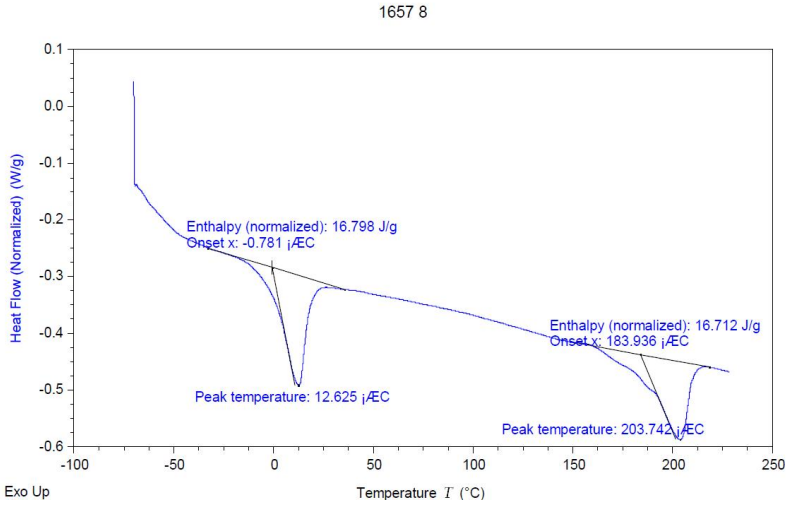

Figure A6 DSC curve of P1/Z8 MMM

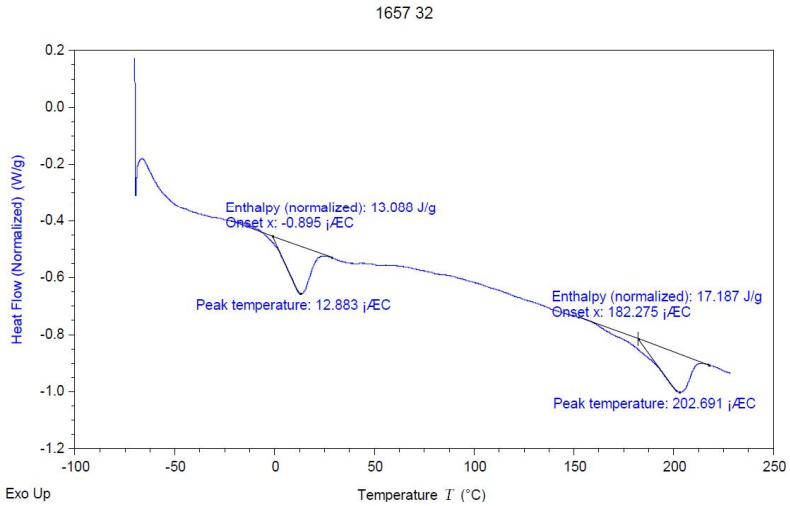

Figure A7 DSC curve of P1/Z32 MMM

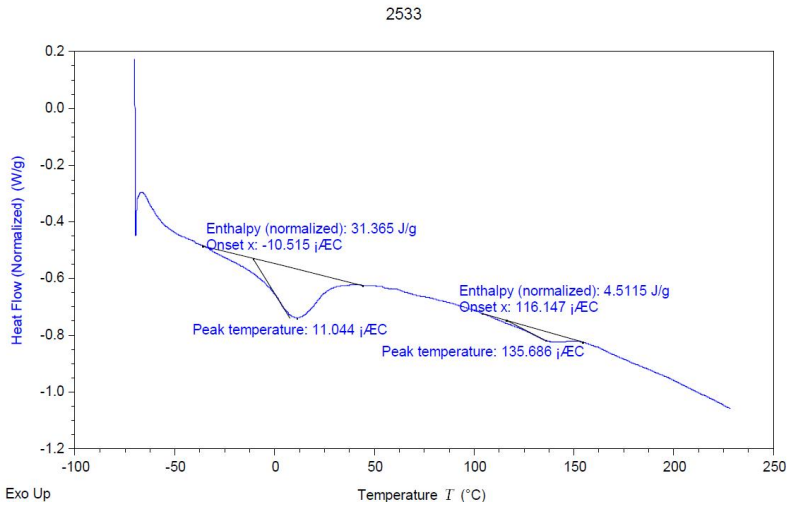

Figure A8 DSC curve of P2

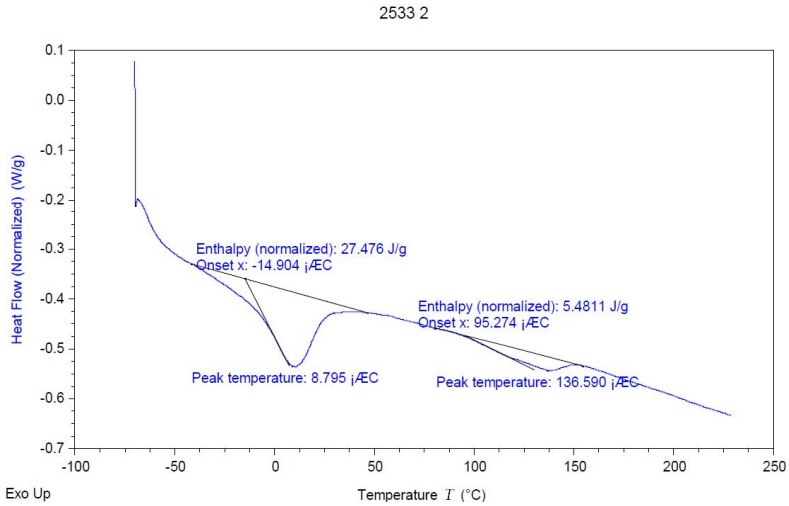

Figure A9 DSC curve of P2/Z2 MMM

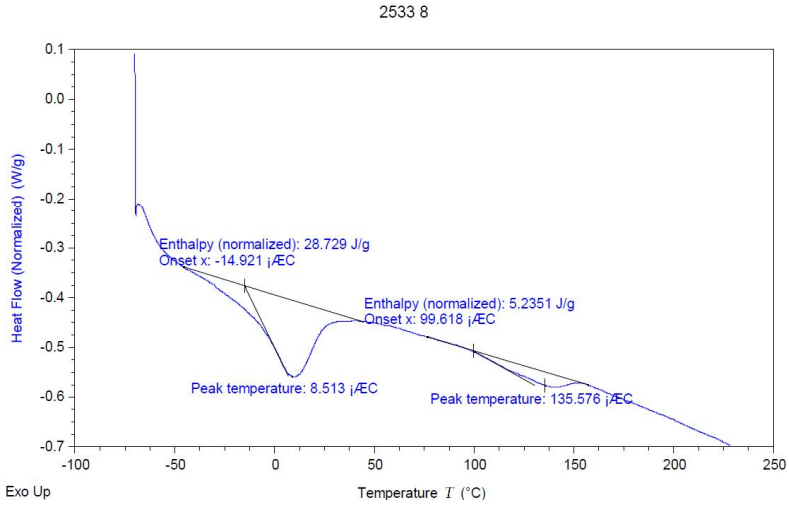

Figure A10 DSC curve of P2/Z8 MMM

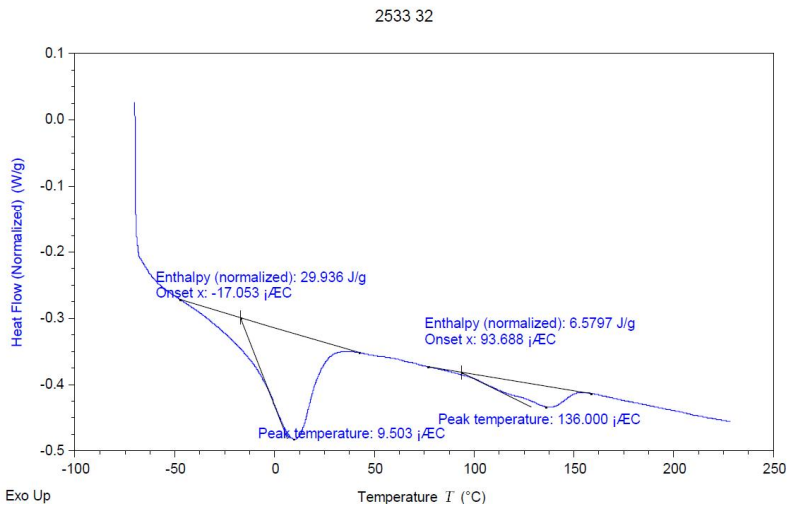

Figure A11 DSC curve of P2/Z32 MMM

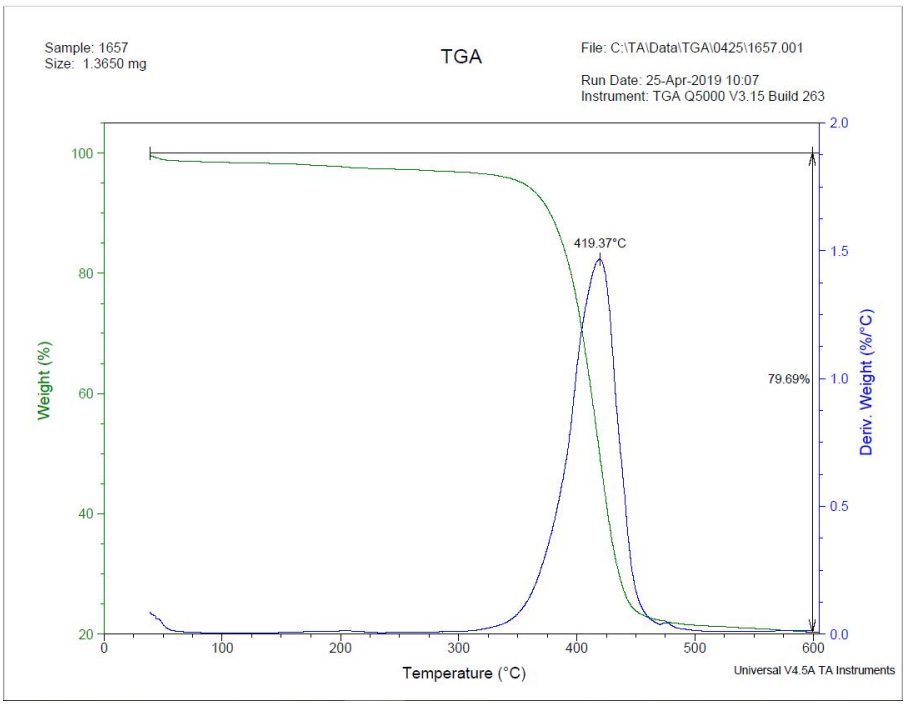

Figure A12 TGA curve of P1

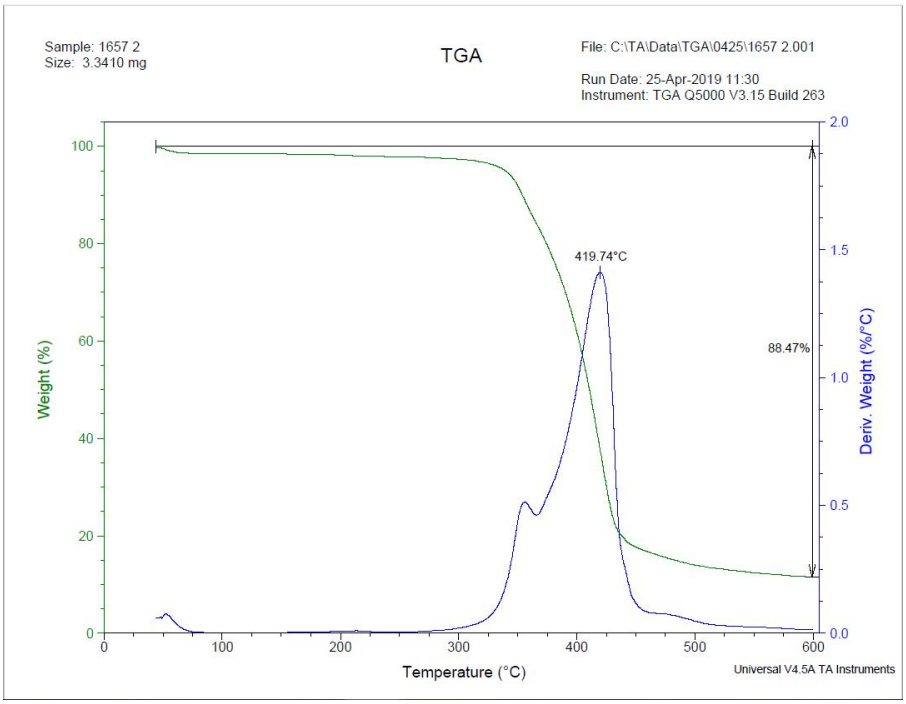

Figure A13 TGA curve of P1/Z2 MMM

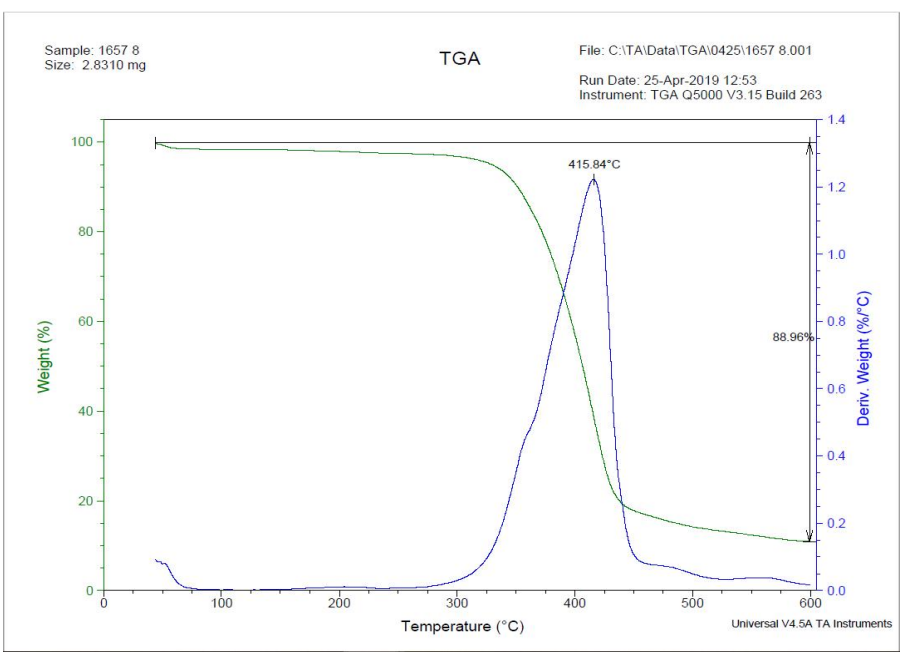

Figure A14 TGA curve of P1/Z8 MMM

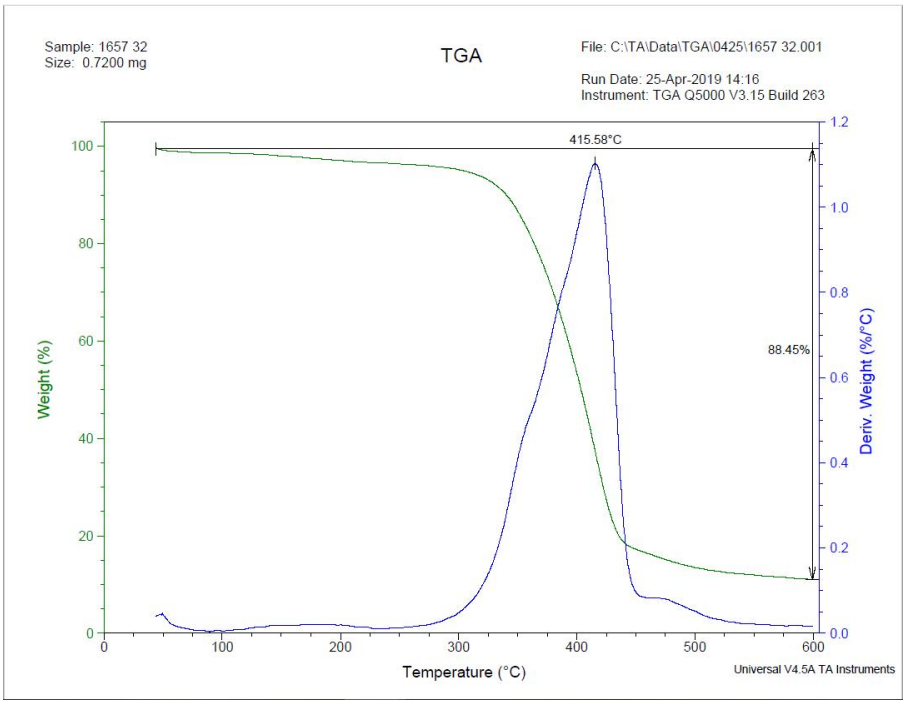

Figure A15 TGA curve of P1/Z32 MMM

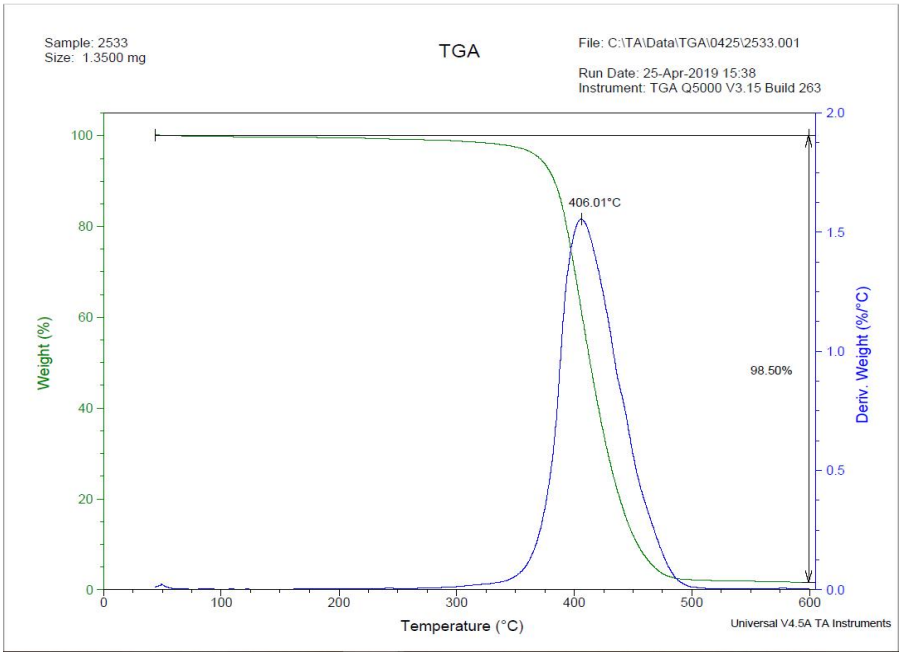

Figure A16 TGA curve of P2

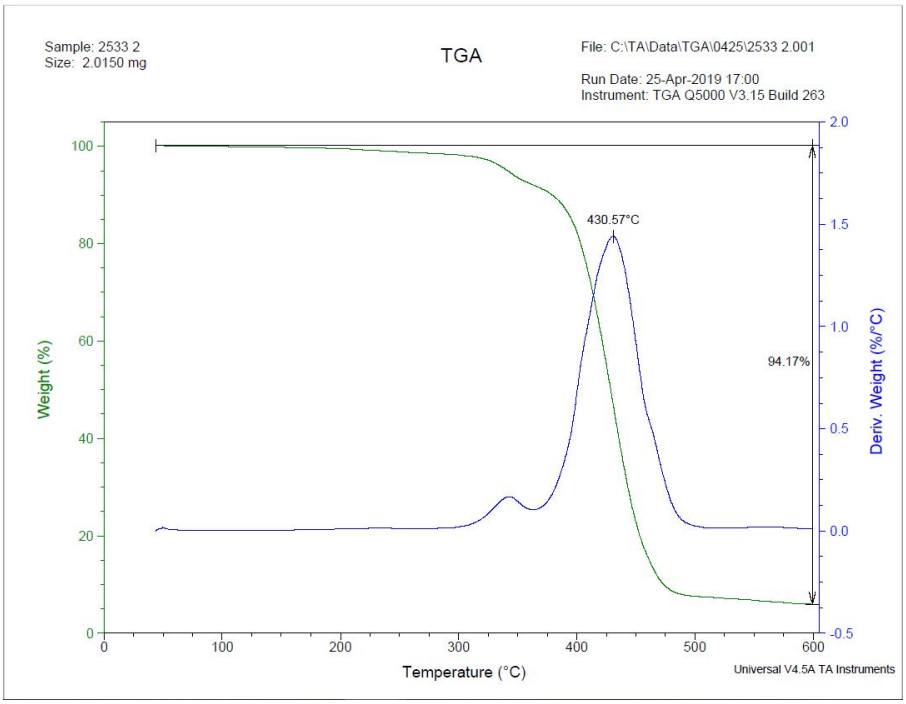

Figure A17 TGA curve of P2/Z2 MMM

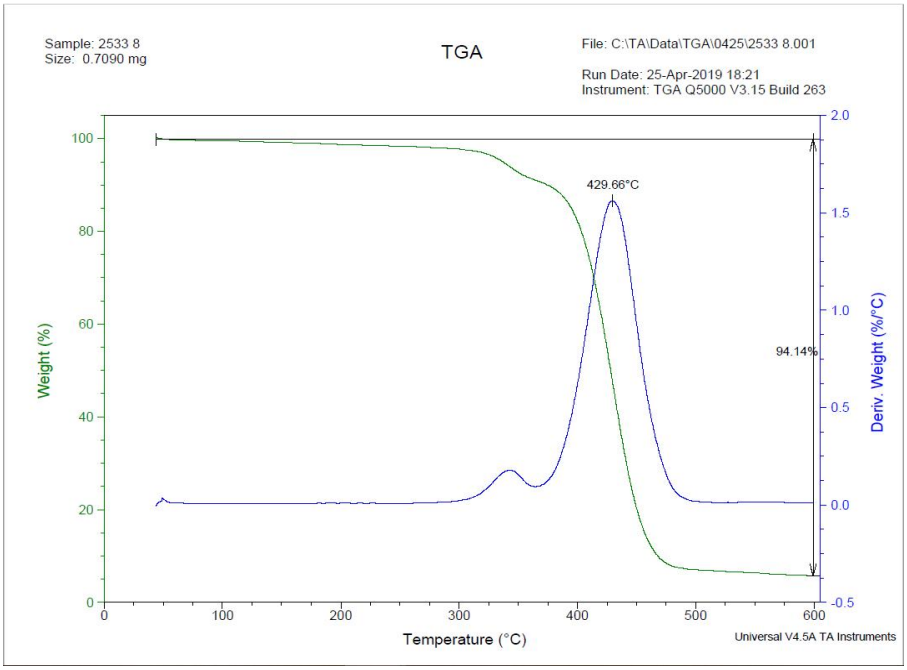

Figure A18 TGA curve of P2/Z8 MMM

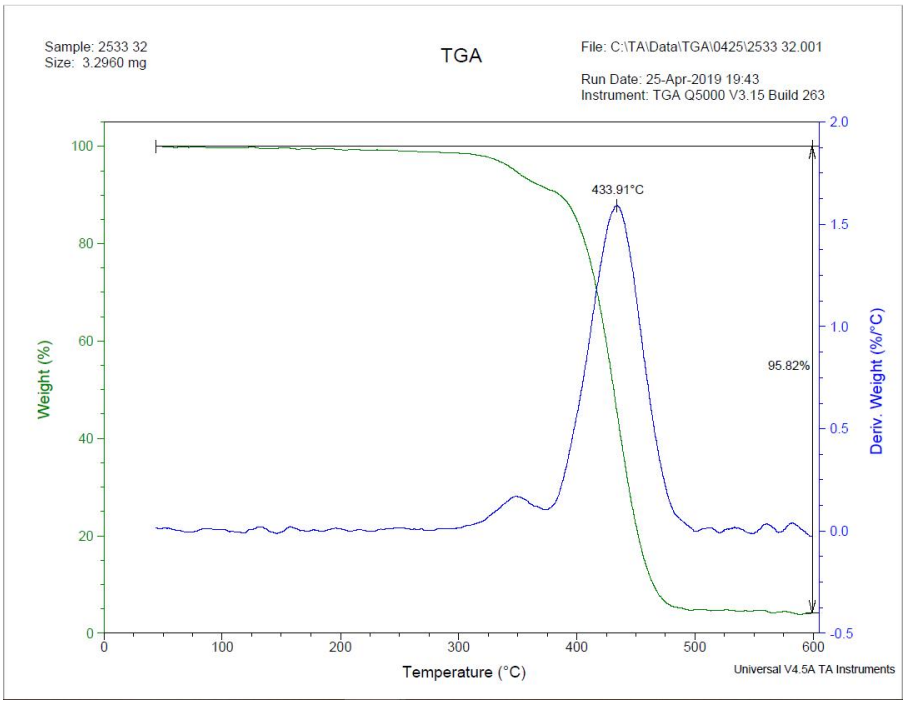

Figure A19 TGA curve of P2/Z32 MMM

초 록

막 기술을 통한 이산화탄소 기체분리의 환경적 · 경제적 이점 때문에 많은 연구가 진행되고 있다. 여러 종류의 막들 중에서, Mixed matrix membranes (MMMs)는 폴리머 막과 무기 물질의 충전재를 결합한 막으로서 기체 투과성과 선택성 모두 향상시키는 결과를 보여주었는데, 이는 폴리머 막의 기체 수송을 개선시킴과 동시에 무기 충전재로 인한 막의 강도의 안정성을 높여주는 장점을 보여준다.

Pebax 1657 막과 Pebax 2533 막에 ZIF-8 의 전구물질인 질산 아연 6 수화물 (zinc nitrate hexahydrate (Zn))과 2-메틸이미다졸 (2-methylimidazole (2-MeIM))의 몰비를 조절하여 MMMs 를 다양하게 조제하였다. ZIF-8 의 전구물질의 몰비는 2-MeIM/Zn 를 2/1, 8/1, 그리고 32/1 로 합성하여 세 가지의 종류의 ZIF-8 을 만들었다. ZIF-8 의 SEM 사진과 XRD 패턴을 통해, ZIF-8 의 전구물질의 몰비를 증가시킬수록 입자의 크기가 작아지고 결정도의 피크도 작아진다는 결과를 볼 수 있었다. 합성된 세가지 종류의 ZIF-8 은 Pebax 1657 과 Pebax 2533 용액 안에 용해한 후 테프론 접시에 부어 72 시간동안 50 °C 에서 캐스팅 시켰다.

전구물질의 몰비가 다른 세 가지 ZIF-8 가 충전되어 있는 Pebax 1657/ZIF-8 과 Pebax 2533/ZIF-8 막을 제조한 후, 이산화탄소와 질소 기체의 투과 실험을 각각 15, 35, 55, and 75 °C 의 온도에서 진행시켜주었다. 같은 온도에서 Pebax 1657/ZIF-8 은 전구물질의 몰비가 32/1 일 때 가장 높은 이산화탄소 투과율을 보여준 반면, Pebax 2533/ZIF-8 은 전구물질의 몰비가 2/1 일 때 가장 높은 이산화탄소 투과율을 보여주었다. 전구물질의 몰비에 따라서 Pebax 1657/ZIF-8 과 Pebax 2533/ZIF-8 의 반대 성향을 보이는 투과율은 Pebax/ZIF-

8 의 XRD 패턴에서 확인할 수 있었다. Pebax 1657/ZIF-8 에서는 ZIF-8 의 전구물질의 몰비가 32/1 일 때 가장 낮은 결정도를 보였고, Pebax 2533/ZIF-8 에서는 ZIF-8 의 전구물질의 몰비가 2/1 일 때 가장 낮은 결정도를 보였는데, 이는 막 안에 결정도가 기체의 투과성에 장애가 되는 요인으로 간주된다.

이산화탄소의 투과성은 Pebax 2533/ZIF-8 이 Pebax 1657/ZIF-8 보다 높은 결과를 보였지만, 이산화탄소/질소 기체 선택성에서는 Pebax 1657/ZIF-8 이 Pebax 2533/ZIF-8 보다 높은 결과를 보였다. 기체의 투과 온도가 높아지는 환경에서는 Pebax 1657/ZIF-8 과 Pebax 2533/ZIF-8 모두 이산화탄소와 질소의 기체 투과율을 향상시켰기 때문에 고온에서의 이산화탄소/질소 기체 선택성이 감소하는 경향을 보여주고 있다.

Pebax 1657/ZIF-8 과 Pebax 2533/ZIF-8 의 이산화탄소 투과성과 이산화탄소/질소 선택성의 다른 결과는 Pebax 1657 과 Pebax 2533 안에 있는 폴리에틸렌 (polyethylene (PE))과 폴리아미드 (polyamide (PA))의 함유량, 폴리머와 ZIF-8 의 화학적 결합의 정도, 및 이산화탄소 친화성의 정도를 비교함으로써 설명할 수 있다. 본 연구에서는 ZIF-8 전구물질의 몰비를 조절하여 Pebax 1657/ZIF-8 과 Pebax 2533/ZIF-8 결합된 막에 이산화탄소 기체를 투과시키는 실험을 진행하였는데, 이는 Pebax 와 ZIF-8 사이의 양립 공존의 중요한 요인을 조사하는 것과 어떤 종류의 폴리머와 무기무질 충전재가 결합되는 것이 이산화탄소의 기체 분리에 있어서 가장 최적인 조건을 밝혀내는데 그 의미가 있다.

주요어: Pebax 1657, Pebax 2533, ZIF-8 몰비 조절, Mixed matrix membranes, 이산화탄소 투과

학번: 2017-22704